博士論文　（要約）

A Study on the Inhibition Mechanism of Halide and Disulfide on the Activity of Polyphenol Oxidase (PPO).

(ハロゲン化物ならびにジスルフィド物によるポリフェノールオキシダーゼの阻害機構)

リム　ジセル　グレース　フェルナンド
Lim, Giselle Grace Fernando

TABLE OF CONTENTS

LIST OF FIGURES

LIST OF ABBREVIATIONS

L-DOPA	3,4-dihydroxyphenylalanine
mPPO	mushroom PPO
Site A	First substrate-binding site of PPO
Site B	Second substrate-binding site of PPO
EoH	PPO empty at Site A and bound to halide at Site B
Eoo	Free PPO
ESH	PPO bound to substrate A at Site A and to halide at Site B
ESo	PPO bound to substrate at Site A and empty at Site B
Cu	copper ion
NMR	Nuclear magnetic resonance
HSAB	Hard and Soft Acids and Bases
CV	Cyclic voltammetry
FWHM	Full width at half maximum
T_1	Longitudinal relaxation time
HEDS	2-hydroxyethyl disulfide
PTU	Phenylthiourea

Chapter 1 Introduction

Polyphenol oxidase (PPO) is a ubiquitous enzyme widely represented in all phyla. It is unique as it can catalyze using two modes of action. It possesses oxygenase activity, wherein the enzyme catalyzes the hydroxylation at the ortho position of monophenolic compounds, and it can also act as an oxidase, catalyzing the subsequent oxidation of the *o*-diphenols to its equivalent quinones (Figure 1.1). The overall reaction results in the concomitant reduction of molecular dioxygen to water. Although PPO exhibits two mechanisms of oxidation, the catalytic action of PPO varies depending on the source from where it was isolated. Most monophenolases may also act as diphenolases, although not all diphenolases possess monophenolase activity (Whitaker, Voragen, & Wong 2003). According to Ramsden and colleagues (2014), the distinction probably depends on the accessibility of potential substrates to the active site. The view that monophenols are first hydroxylated at the ortho position, forming a diphenol intermediate that is further oxidized to *o*-quinone is common in literature. However, it was also suggested that the monooxygenase reaction of PPO allows phenols to be directly oxidized into the quinone, and a diphenol intermediate is unnecessary (Ramsden et al., 2014).

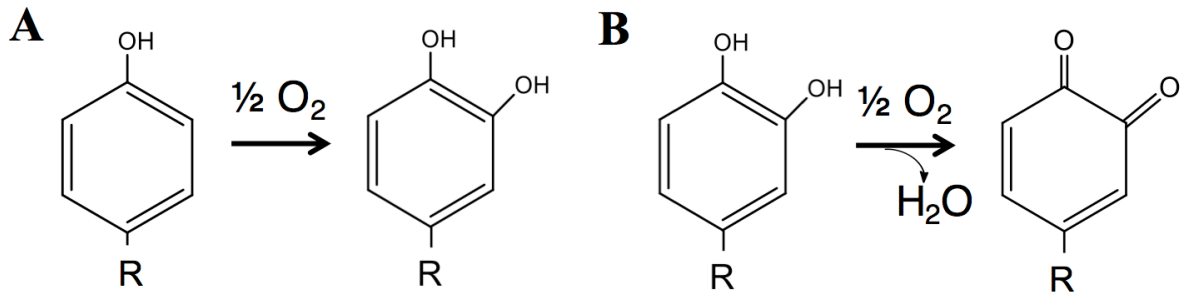

Figure 1.1 Two mechanisms of oxidation for polyphenol oxidase (PPO).
It is involved in the oxygenation reaction of monophenols to form diphenols (A). It can also act as a diphenolase, catalyzing the oxidation of *o*-diphenols to *o*-quinones (B).

The enzyme has been identified and isolated in a wide number of phyla including plants (Lourenco, Neves, & Da Silva, 1992; Eicken et al., 1998; Halder, Tamuli, & Bhaduri, 1998; Murao et al., 1993; Rompel et al., 1999; Janovitzklapp et al., 1990; Paul and Gowda, 2000; Mari et al., 2003; Unal, 2007; Zheng, Shi, & Pan, 2012; Virador et al., 2010; Manohan, 2012; Rompel et al., 2012), animals (Martinez et al., 1986; Zheng, Shi, & Pan, 2012, Laino et al., 2015), fungi (Halaouli, 2004; Gouzi, Gaouar, & Benmansour, 2008), and microrganisms (Lerch, 1983; Woolery et al., 1984). As mentioned earlier, the catalytic action of PPO depends on the source from where it was isolated. To more accurately classify the enzyme, it

has been referred to in literature by various names, corresponding to its mode of activity. As such, cresolase is used to refer to enzymes with monooxygenase activity while the terms catecholase or catechol oxidase are used if the enzyme catalyzes only the oxidation of diphenols to quinones. In other papers, the term tyrosinase is referred to enzymes that are assumed to possess both monooxygenase and diphenolase activity (Marusek et al., 2005; Lee and Whitaker, 1995; Kaintz et al., 2014). To prevent ambiguity, the term polyphenol oxidase (PPO), referring mostly to the diphenolase activity, will be used throughout the discussions in this paper.

PPO as a type- 3 copper metalloprotein

PPO belongs to the group of enzymes classified as copper metalloenzymes, owing to the presence of copper at its active site. Copper metalloenzymes are classified into three types, according to their structure and spectroscopic properties. Type 1 "blue copper" oxidases have one copper atom in the active site and it is mostly involved in electron transfer. Type 2 copper centers are commonly found in enzymes that activate molecular oxygen. Lastly, type 3 copper metalloenzymes are characterized by its binuclear copper center, and its mode of action is in the activation of molecular dioxygen. The most well-known members of this type are the tyrosinases, catechol oxidases, aureusidin synthase and hemocyanins (Kaintz, Mauracher, & Rompel, 2014).

The structure of the binuclear copper center in type 3 proteins is well characterized, owing to crystal structures of some PPOs that have been elucidated to date. Examples of crystal structures available in literature are from sweet potato catechol oxidase (Klabunde et al., 1998), from grape catechol oxidase (Virador et al., 2010) and from tyrosinase from *Agaricus bisporus* (Ismaya et al., 2011). In the binuclear copper center, each of the copper atoms is bound to three histidine residues at the N-ε (Bubacco et al., 1999; Ismaya et al., 2011). In mushroom PPO, the ligands of the first copper ion, termed CuA is bound to His61, His85, and His94. The second copper ion, CuB, is bound to His259, His263, and His296 (Ismaya et al., 2011). Oxygen is bound in a peroxy "side on" bridging mode, resulting in the activation of dioxygen and giving rise to the characteristic features of this type of protein such as: 1) strong antiferromagnetic coupling between the two s=1/2 copper ions due to covalent overlap with a bridging ligand, resulting in the absence of an electron paramagnetic resonance (EPR) signal; 2) a Raman-active O-O stretching vibration at 750 cm^{-1} and 3) absorption features

unique as when compared to simple copper complexes: an intense band at 345 nm (ε = 19,000 cm^{-1} M^{-1}) and another reasonably intense band at 600 nm (ε=1000 cm^{-1} M^{-1}) (Himmelwright et al., 1980; Decker et al., 2007; Klabunde et al., 1998; Eicken et al., 1998, Rompel et al., 1999). It is interesting to note that the dual action of oxygenation and oxidation exhibited by PPO is attributed to the two copper atoms of the active site (Ramsden and Riley, 2014).

The different oxidation states of the copper center of PPO

The copper (Cu) ions in the active site are thought to be directly involved in the catalytic functions of PPO. Alignment of amino acid sequences of PPO from different organisms show very low homology (Kaintz et al., 2014), except for a few conserved amino acid sequences (Figure 1.2). From site-directed mutagenesis, it was known that these conserved regions account for the histidine residues that coordinate with the metal ligands (Klabunde et al., 1998; Jackman et al., 1991). Therefore, it is understood that the copper-binding domain is highly conserved among all organisms, plays a fundamental role in PPO structure and activity (Lee and Whitaker, 1995; Bubacco et al., 2000; Oliveres et al., 2002).

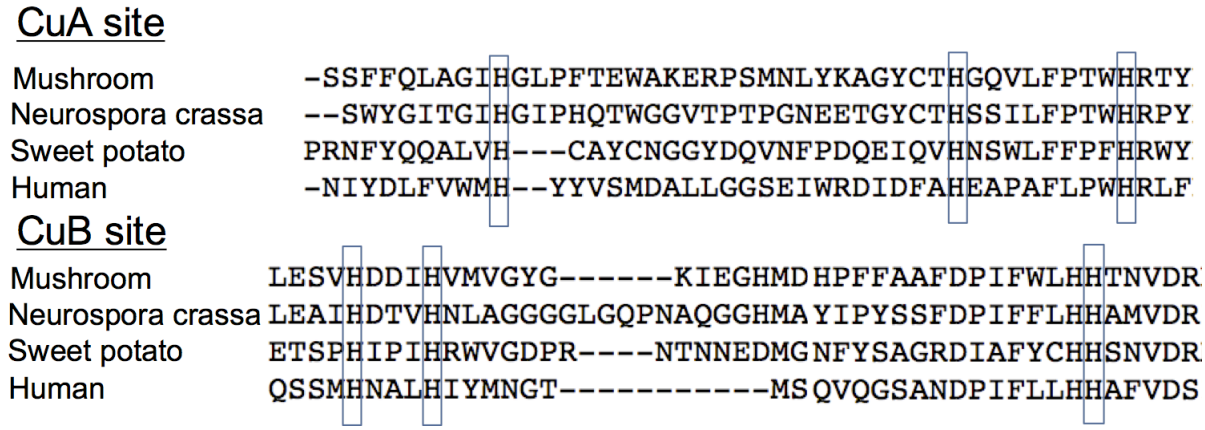

Figure 1.2 Conserved copper-binding domain in tyrosinase.
Amino acid sequence alignment of mushroom tyrosinase, *Neurospora crassa* tyrosinase, sweet potato catechol oxidase and human tyrosinase. The histidine residues ligating the two copper ions (CuA and CuB) are enclosed in boxes.

Copper, being an electroactive species, may exist in at least two oxidation states in biological systems. During enzyme activity, the oxidation states of copper change to give different forms of the enzyme. The following copper oxidation states have been reported:

i) *met* Cu(II) Cu(II) form

The favorable redox potential of the met form, as well as its stability, make it the predominant form in the resting enzyme (Ramsden and Riley, 2014; Rompel et al., 1999). This form adopts a tetrahedron conformation, with copper located at the apex. The three other apices are formed by the three His nitrogen atoms and a hydroxide ion most probably forms a bridge between the two metal ions (Rescigno et al., 2002). According to Sanchez-Ferrer et al., this redox form of PPO is unable bind molecular oxygen and also cannot act on monophenols (Sanchez- Ferrer et al., 1995). On the other hand, this form shows higher affinity to diphenol substrates (Ramsden and Riley, 2014). The met-form maintains Cu in the +2 state and a bridging ligand connects the two ions. More often, the bridging ligand is a hydroxyl molecule (Ramsden and Riley, 2014; Rescigno et al., 2002).

ii) *deoxy* Cu(I) Cu(I) form

In the deoxy form, Cu is found as a cuprous ion, the arrangement of which is similar to the met form, only without the hydroxide bridge (Rescigno et al., 2002). This is the only form capable of binding and activating molecular oxygen, consequently being converted to oxy-PPO (Sanchez-Ferrer et al., 1995).

iii) *oxy* Cu(II)-O-O-Cu(II) form.

In the oxy form, dioxygen is bound between the copper ions via a peroxy μ-η^2: η^2 configuration, or a side-on bridging coordination between the copper atoms (Decker et al., 2007). It is also referred to as the active form or primary oxidizing form of PPO (Ramsden and Riley, 2014). Because of the high electron density at the peroxide σ^* orbital, the O-O bond is weak and readily cleaved (Rescigno et al., 2002; Sanchez-Ferrer et al., 1995). The oxy-form is also considered as the intermediate that links the two different activity mechanisms of PPO. In the presence of dioxygen, both monophenol and diphenols are oxidized by oxy-PPO to *o*-quinones, albeit occurring by separate oxidative cycles (Ramsden and Riley, 2014). Often, a greater affinity to diphenols compared to monophenols is exhibited by oxy-PPO (Ramsden and Riley, 2014).

Most studies would describe only three oxidation states for the PPO dinuclear copper center. However, a paper by Ramsden and Riley described a fourth possible oxidation state: *deact-*

tyrosinase (Ramsden and Riley, 2014). In this situation, a diphenol is occassionally treated as a monophenol and is oxidized in a monooxygenase mechanism by oxy-PPO. As a result, one of the copper atoms is reduced to the Cu (0) state and may diffuse out of the active center, leading to the eventual inactivation of the enzyme (Ramsden and Riley, 2014).

Monophenolase and diphenolase activity of PPO

What makes PPO an interesting enzyme is its ability to perform two oxidation reactions on different substrates. It acts on monophenol in an oxygenation reaction. At the same time, it can also use diphenolic compounds as substrates, oxidizing them to the corresponding quinones. Differences in K_s and *Kcat* values indicate that the oxidation reactions occur faster than the oxygenase step (Rescigno et al., 2002). The discrimination between monophenolase or diphenolase occurs by virtue of the different affinities of substrates to each redox state of the active site copper (Wilcox et al., 1985). For example, the inability of the met form to bind dioxygen makes it incapable of monophenolase activity, rendering the binding of monophenolic substrates limited to only oxy-PPO. On the other hand, this discriminatory binding to PPO does not occur for the diphenolase cycle. It is the interconversion of these different oxidation states that explains the unusual kinetic features of the enzyme. Particularly, in PPO, the changes in the valency are induced by dioxygen or substrate binding to the two copper atoms (usually termed CuA and CuB) in the active site. Ramsden and Riley provided an excellent description of the changes in the copper oxidation accompanying the steps of the oxidation reaction (Ramsden and Riley, 2014). Although in this study, focus is given to only the diphenolase activity of PPO, it is worthwhile to also mention the monooxygenase action of PPO. A brief summary of the different PPO states is presented here:

a. Oxy-PPO to deoxy-PPO conversion: The oxidation of phenols to *o*-quinones
   The oxygen of the phenol binds to CuA, followed by electrophilic monooxygenation to make the substrate bound to both copper ions. A homolytic dissociation gives the ortho-quinone and deoxy-PPO. The deoxy-PPO can bind oxygen to change to oxy-PPO to continue the catalytic cycle (Figure 1.2 A).

b. Oxy-PPO to met-PPO conversion: The oxidation of catechol to ortho-quinones
   Although oxy-PPO can bind both monophenols and diphenols, a higher specific activity for catechol oxidation has been observed. This may be due to the difference in the ease

of substrate binding to the active site. In this reaction, catechol initially binds to CuB. The adjacent hydroxyl groups of the substrate are first deprotonated to coordinate with the two coppers. In the process, oxy-PPO changes to the met form. The substrate-enzyme complex dissociates into an *o*-quinone and one oxygen in the peroxy configuration is released as water. The remaining met-PPO still has oxygen bound to it, probably in the hydroxyl form. A second catechol molecule may bind for oxidation to a second *o*-quinone. Concomitantly, Met-PPO copper is reduced to deoxy-PPO with Cu(I) oxidation state (Figure 1.2 B). Cu(II) is restored by binding dioxygen.

c. Met-PPO to deoxy-PPO conversion: autoactivation and the lag period

This step explains the observed lag period during the monooxygenation reaction. Monoxygenation starts with the binding of oxygen to Cu(I). However, the redox potential of copper prefers the Cu(II) state which is unable to bind molecular oxygen. Although the phenolic substrate can bind to the active site, oxygenation cannot ensue without oxygen binding. For the reaction to proceed, Cu(II) is converted to Cu(I) through reduction by a diphenolic substrate. In the native form of PPO, some amounts of oxy-PPO are present. This can generate small amounts of *o*-quinones. Nucleophilic addition to the ortho-quinones produces the catechols necessary for the Cu(II) conversion. The lag period observed in the monoxygenation cycle is accounted for by the time required for small amounts of catechol to be formed. In some experiments, the lag time is remarkably decreased by adding small amounts of catechol or added reductants at the start of the reaction (Rescigno et al., 2002).

The interconversion of PPO from oxy-PPO to the deactivated form, although presented in literature, will not be mentioned here.

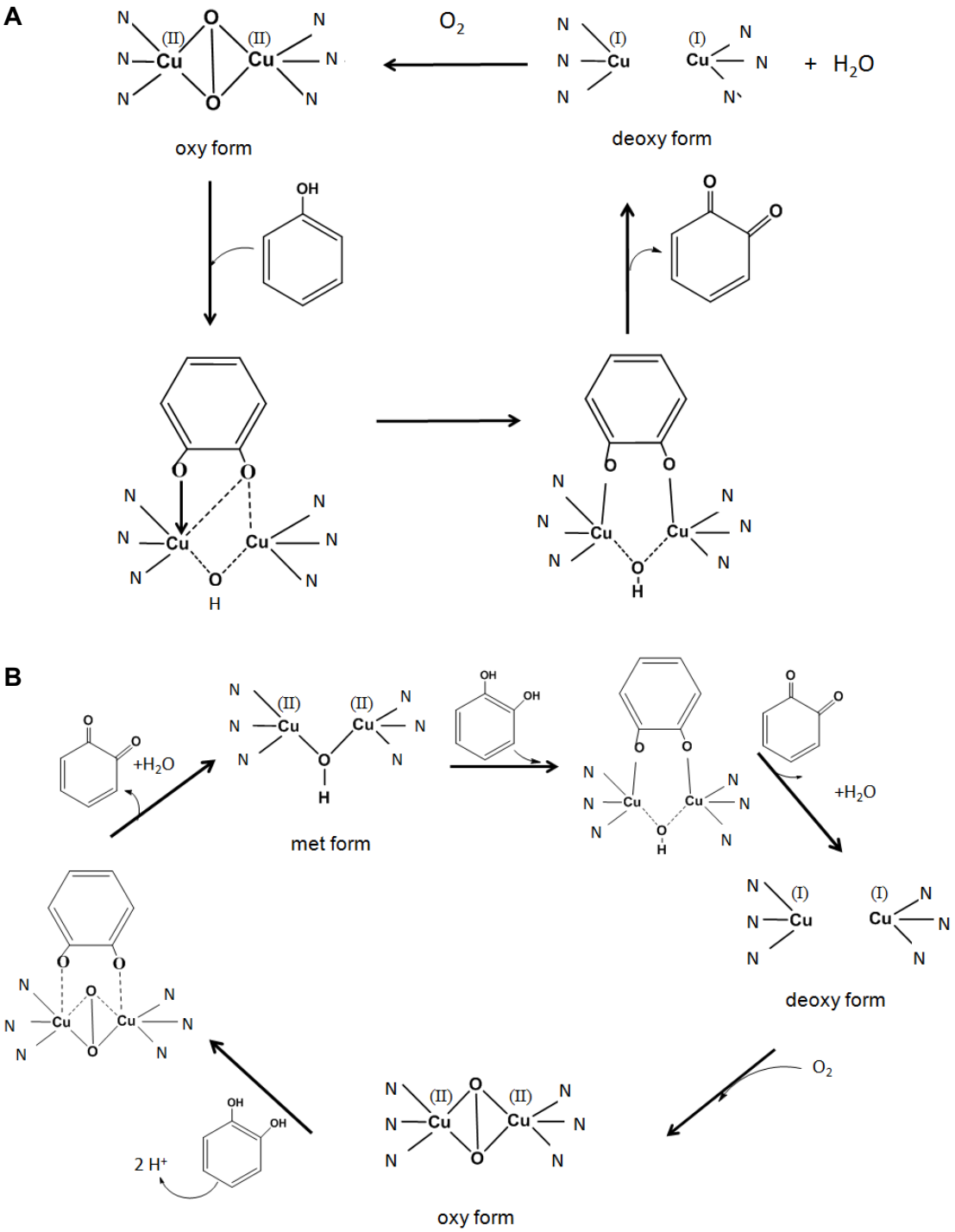

Figure 1.3 Reaction mechanisms of the monophenolase and dipehenolase activity of PPO. The monophenolase (A) and diphenolase (B) activity of PPO is described. The copper ions in the active site are directly involved in the catalytic cycle. The affinity of the substrate depends on the redox state of the active site copper. Monophenols can bind only to the oxy-form of the enzyme while diphenol substrates are able to bind to both met- and oxy-PPO. The scheme is adapted from the mechanism presented by Ramsden and Riley (2014).

Similarities and Differences with Hemocyanin

Information on the crystal structures of plant and fungal PPO were not available until recently. For many years, the understanding of PPO structure relied heavily on information from the study of another similar type-3 copper protein, hemocyanin. Hemocyanins are found in the hemolymph of molluscs and arthropods where they are responsible for the precise delivery of oxygen to different tissues (Rescigno et al., 2002). It is similar to PPO as both enzymes contain a binuclear copper unit and both reversibly bind oxygen (Himmelwright et al., 1980). From X-ray studies, it was suggested that the conformation change that occurs among the different redox forms of PPO is strictly parallel with hemocyanin (Rescigno et al., 2002). Further, the active sites of PPOs and hemocyanins with oxygen bound to the copper atoms have similar spectroscopic properties such as UV-resonance Raman and UV-Vis (Decker et al., 2007; Himmelwright et al., 1980). Despite the similarities in active site structure assumed for the two copper proteins, their functions and other structures vary widely. While polyphenoloxidases are identified as catalysts of oxidation reactions, the function of hemocyanins is limited to oxygen transport. The group of Decker (2007) presented a comprehensive review comparing the structural features activity of PPO and hemocyanins (Decker et al., 2007). It is frequently mentioned that the difference in function of the two proteins lies in the active site structure. Hemocyanin active site contains a bulky amino acid, usually phenylalanine or tyrosine, which is not common in PPO. This bulky residue acts as a shield of the active site, making it inaccessible to phenolic substrates, preventing activity (Decker et al., 1998). It is worthwhile to mention, however, that some studies on hemocyanin structure research suggest that hemocyanins can be activated to act as catalysts. Salvato et al. were able to isolate hemocyanins with *o*-diphenolase activity from octopus (Salvato et al., 1998) while individual studies by of Zlateva, Nagai, and Pless present that hemocyanins from various arthropods could also catalyze oxidation reactions (Zlateva et al., 1996; Nagai, Osaki, & Kawabata 2001; Pless et al, 2003). The conversion of the oxygen-carrier to an active catalyst occurs as a result of limited proteolysis with trypsin or chymotrypsin, or by SDS treatment. These treatments either remove a domain fragment including the amino acid clog, or induce a conformation change to make the active site more available to accept the phenolic substrate (Decker et al., 1998; Adachi et al., 2001; Decker et al., 2001; Soderhall et al., 1998). In arthropods, the active site is covered by a phenylalanine residue while for bacteria *Streptomyces* tyrosinase, it is covered by a tyrosine residue. For molluscan hemocyanins, hydrophobic amino acids such as

leucine frequently close the active site, preventing the binding of substrate (Marusek et al., 2006). This process of activation is not limited to hemocyanins and a similar phenomenon was described for a latent PPO from sweet potato cells which required activation by SDS treatment (Nozue et al., 1999). Similarly, broad bean leaf PPO that was latent when purified was activated after proteolytic cleavage of a 15 kDa protein from the C- terminal (Robinson and Dry, 1992).

Biological Functions of PPO

Many studies have described the biological activities of PPO but a definite function is yet to be established. It is suggested to be involved in wound healing in plants and arthropods (Decker, 2007). Further, due to the fungistatic, bacteriostatic, and anti-viral properties of PPO, it plays a role in the primary immune response of arthropods and other invertebrates (Decker et al., 2007; Soderhall et al., 1998). Some authors also mentioned that the quinone products of PPO oxidation can sclerotize the protein matrix of the arthropod cuticle after molting (Decker et al., 2007; Andersen et al., 1996).

In mammals, PPO is identified with melanin formation. Melanin synthesis begins with the common precursor, L-tyrosine, being converted to dopaquinone via a monooxygenase reaction catalyzed by PPO. By a succeeding series of steps, dopaquinone is ultimately converted into intermediates that react with other compounds to form the pigment compounds. The oxidation step catalyzed by PPO is the fundamental step in melanosynthesis, as evidenced by the albinism that occurs in the absence of the enzyme (Ramsden and Riley, 2014; Mendes, Perry, & Francisco, 2014).

The reactions of PPO are also important in agriculture. In food, it produces the coloration desirable for coffee, tea, and cocoa (Martinez and Whitaker, 1995). On the other hand, it is also responsible for the undesirable discoloration in fruits and vegetables caused by damage during handling, storage, and processing (Queiroz et al., 2008). It catalyzes the oxidation of phenolic compounds innate in fruits and vegetables, converting them to benzoquinones. The benzoquinones react rapidly, polymerizing non-enzymatically to form the highly colored melanin pigments normally equated to senescence (Figure 1.4). In intact products, the skin and other waxy substances keep out dioxygen. However, when fruits and vegetables are bruised or sliced, dioxygen freely enters, hastening browning. This reaction decreases the

marketability as well as the nutritional value of the products. As much as 50% of harvests are lost for consumer consumption, translating to huge losses in profits and in food supply (Lee and Whitaker, 1995).

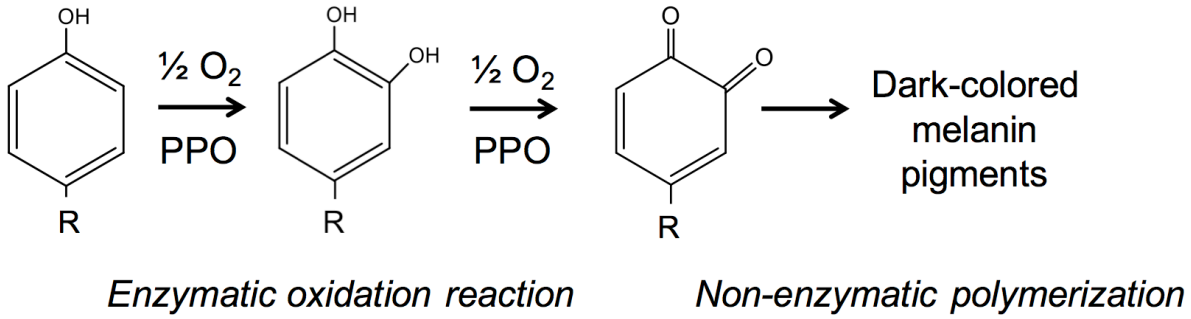

Figure 1.4 The synthesis of melanins as a product of PPO oxidation.
One of the important reactions of PPO is the oxidation of phenolic compounds that are precursors to melanin synthesis. The quinone products of oxidation react with other proteins or polymerize with each other non-enzymatically to form dark-colored pigments. The type of pigment produced depends on the starting phenolic precursor.

Applications of PPO in Environment and Food Safety

The reactions of PPO have an advantageous application especially in environmental analysis and food quality monitoring. In the environment, PPO plays a vital role in detoxifying soils of xenobiotics introduced to the environment by irresponsible release of industrial waste or by excessive use of pesticides. A paper by Park and colleagues (Park et al., 1999) describes the mechanism of soil detoxification mediated by phenoloxidases. These enzymes that are naturally found as humic constituents mediate the transformation of the xenobiotics, leading to their detoxification. The mode of action of enzymes in detoxification follows this process: First is the enzyme- catalyzed oxidation of chlorophenols to free radicals or quinones. Then, these products of oxidation undergo chemical coupling. The xenobiotics may couple with each other and precipitate out of the solution or it could couple to humus, resulting in formation of covalent linkages (Park et al., 1999). In a similar application, Loncar and Vujcic´(2011) developed tentacle carriers with immobilized potato phenoloxidase for application of halogenophenol removal from aqueous solutions. By covalently linking the PPO to a matrix support, they were able to introduce a more economical xenobiotic removal in wastewater treatment (Loncar and Vujcic´, 2011).

Phenols are also commonly used in agricultural products as harmful germicides and pesticides. As such, methods are constantly being developed in order to monitor the quality of food. The current practice uses gas chromatography and spectrophotometry. In recent technology, the use of enzymes is gaining popularity because of its low cost and safety. Enzyme-based biosensors for detection of phenolic compounds are being developed and most of these biosensors use tyrosinase immobilized on different electrode supports. As further improvement, nanostructures as electrode supports are being developed. Nanostructures have large specific surface area and have high total porosity, allowing high enzyme loadings and efficient transport of analytes through the membrane toward the electrode surface (Arecchi et al., 2010). Arecchi et al., reported of a nanofibrous membrane-based tyrosinase biosensor for the detection of phenolic compounds in foods (Arecchi et al, 2010).

Clearly, from the point of view of economics and biosafety, enzymes such as PPO offer a more sustainable alternative for food quality check, soil cleanup and wastewater treatment.

Inhibition of PPO activity

In contrast to the beneficial effect of PPO in the environment, this enzyme is associated with detrimental effects in aesthetics and in the food industry. As mentioned above, PPO is the main culprit behind skin pigmentation by catalyzing the first two steps of melanin formation: the hydroxylation of tyrosine to L-DOPA and the succeeding two-electron oxidation of L-DOPA to dopaquinone. The next oxidation steps following these ultimately produce melanins that are undesirable from the point of view of aesthetics (Mendes, Perry, & Francisco, 2014).

The reactions of PPO are also an area of concern in food and agriculture because it produces the dark-colored pigments equated to food senescence, decreasing its nutritional value and marketability. In plants, phenolic compounds are naturally found as these substances contribute to the organoleptic properties of food (Queiroz et al., 2008). Plant PPOs are located in the lumen of the thylakoid membranes in chloroplasts while the phenolic compounds are freely located in the cytosol (Kaintz, Mauracher, & Rompel, 2014). When plants are damaged in handling and storage, the compartments separating the two compounds are disrupted, allowing their reaction that results in undesirable browning. In addition, when fruits are bruised or sliced, the skin and other waxy substances are destroyed, dioxygen freely

enters, and browning is further hastened (Queiroz et al., 2008). Because of the detrimental effects of PPO to economics, food security, and aesthetics, many efforts are being undertaken to control its reactions.

The basic principle in any enzyme inhibition efforts involves the following: a) direct inhibition or inactivation of the enzyme; b) elimination or transformation of the substrate to an unreactive form or c) a combination of both a and b (Vamos-Vigyazo, 1995). Traditional methods are various, ranging from non-chemical treatments to the addition of chemical inhibitors. Heat treatment such as blanching is the most widely used in stabilizing food by its ability to inactivate enzymes. Treatment of food at boiling temperatures for few minutes can destroy microorganisms and denature the detrimental enzymes. Although effective in preserving food color and quality, this method can cause the loss of vitamins, thermosensitive nutrients, and other water-soluble components (Vamos-Vigyazo, 1995; Queiroz et al., 2008; Seo, Sharma, &Sharma, 2003; Severini et al., 2003). Other non-chemical treatments include high hydrostatic pressure treatment, gamma irradiation, sonication, and application of a pulsed electric field. These methods commonly aim to inactivate the protein by inducing conformation changes or by denaturation (Vamos-Vigyazo, 1995; Queiroz et al., 2008).

Despite the non-chemical treatments available, it is still popular to use chemical inhibitors in the control of PPO oxidation. These effectors act on one or more of the essential components of PPO reaction: oxygen, copper, substrate, or the enzyme itself. Sulfating agents were widely used until alarms on its adverse health effects were raised by the World Health Organization (Queiroz et al., 2008). However, another sulfated compound, cysteine, can prevent color development by trapping the quinones as colorless addition products (Richard-Forget, Goupy, & Nicolas, 1992; Vamos-Vigyazo, 1995). Ascorbic acid (AA) and citric acid (CA) are also commonly used inhibitors. It is thought that AA helps prevent enzymatic browning by reducing the ortho-quinones formed back to the original catechol. This step prevents the further formation of the colored pigments, but does not directly inactivate PPO. AA also works by lowering the pH, where PPO gets denatured. CA works similarly by decreasing the pH (Queiroz et al., 2008; Vamos-Vigyazo, 1995; Pizzocaro, Torreggiani, & Gilardi, 1993).

Copper chelators are regarded as “true” inhibitors because their binding directly inactivates PPO. Many of these compounds are effective inhibitors but an exact mechanism applicable

for all is yet to be stated. Inhibition depends on the redox state of the PPO active site, and the coordination chemistries are sharply different for the cuprous and cupric ions (Rescigno et al., 2002). Kojic acid (5-hydroxy-2-hydroxymethyl-4-pyrone), the antibiotic by-product of rice fermentation, is an example of a copper-chelating inhibitor. It can bind to the di-copper center but is not acted on by PPO. Furthermore, it decreases oxygen uptake by the enzyme. In literature, it is described as a slow-binding competitive inhibitor (Lee and Whitaker, 1995; Chen, Wei, & Marshall, 1991; Chen et al., 1991; Kahn, Lindner, & Zakin, 1995), popularly used a whitening agent in cosmetics and is also used to prevent oxidative browning in shrimp (Chen et al., 1991). Other examples of copper chelators in literature are tropolone, hydroxamic compounds, and hydrazine derivatives (Vamos-Vigyazo, 1995; Chen and Kubo, 2002; Rescigno et al., 2002; Seo, Sharma, & Sharma, 2003; Queiroz et al., 2008; Mendes, Perry, & Francisco, 2014). Synthetic copper chelators such as phenylthiourea have also been presented (Klabunde et al., 1998; Mendes, Perry, & Francisco, 2014).

Substrate analogs also competitively inhibit PPO activity. The most common examples of this type of inhibitors are resorcinols. Resorcinol, or *m*-dihydroxybenzene, has a good inhibition effect and its efficacy can be modified by the addition of substituents to the parent compound. For example, 4-hexylresorcinol proved to be a more potent inhibitor and is currently used to prevent browning in shrimp (Loizzo, Tundis, & Menichini, 2012; Dawley and Flurkey, 1993). Benzoic acid and other carboxylic acids are also famous inhibitors and are classified as competitive inhibitors of the enzyme because of its close structural resemblance to the substrates (Rescigno et al., 2002). Modifications to substrates, such as glycosylation, may also be used for preserving food quality (Vamos-Vigyazo, 1995).

Small ligands, such as cyanide, azide, and halides, are known to be capable of binding to copper. They are thought to inhibit PPO by acting as purely competitive inhibitors of dioxygen binding although other mechanisms have also been proposed (Rescigno, 2002).

A summary of the various known PPO inhibitors, including its structure and mode of action, are presented in Figure 1.5.

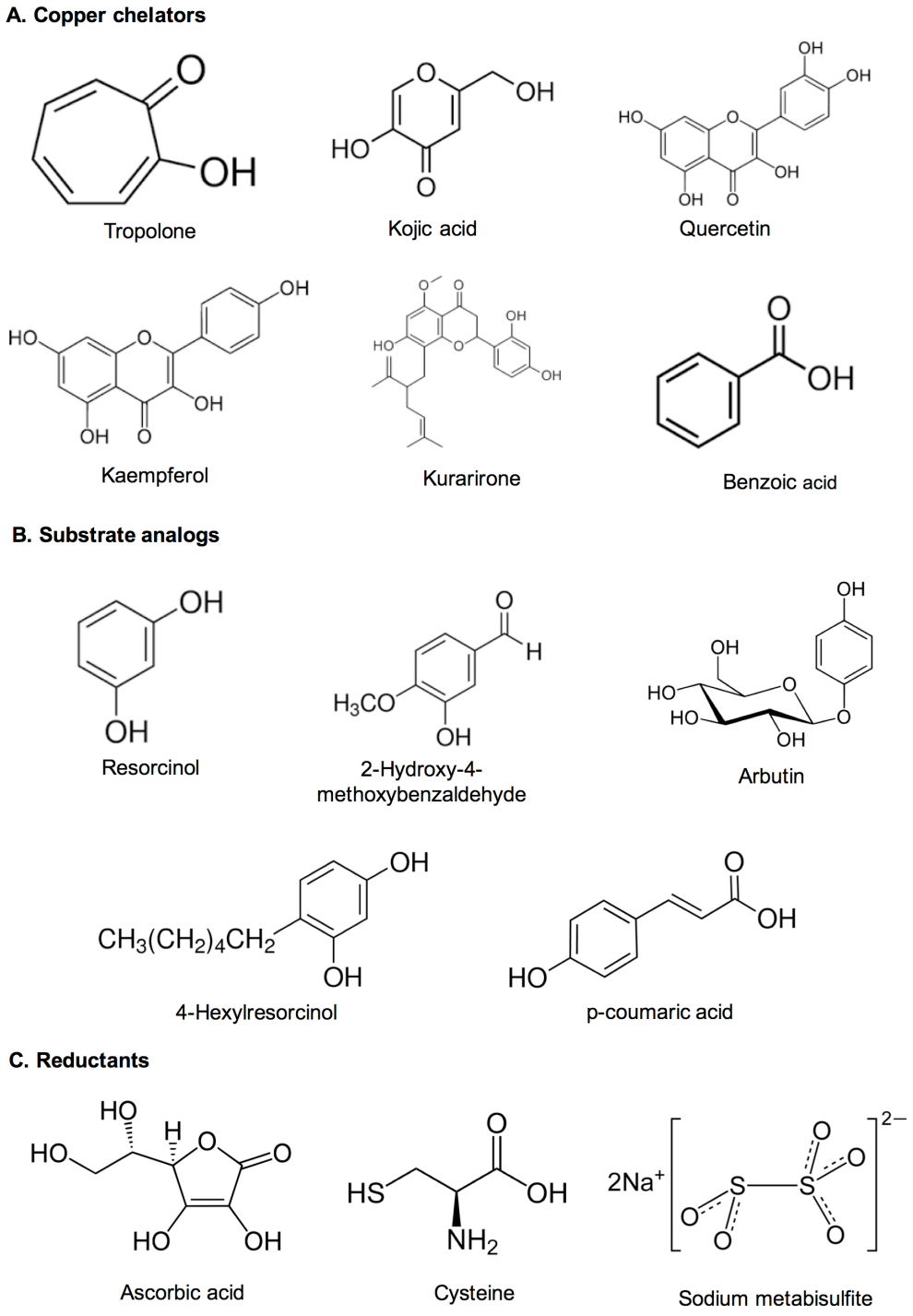

Figure 1.5 Some common inhibitors of polyphenol oxidase and their corresponding modes of action.

Another developing study in PPO inhibition is the extraction of natural inhibitors from plants. These compounds hold promise in food and cosmetic applications because it offers satisfactory efficacy and is mostly free from harmful side effects compared to its synthetic counterparts (Seo, Sharma, & Sharma, 2003; Loizzo, Tundis, & Menichini, 2012). Plant-derived PPO inhibitors mentioned to date are mostly flavonoids, where the 4`hydroxyl

substitution is required for inhibition. Aldehydic compounds, because of their ability to form Schiff bases with PPO residues, also contribute to inhibition. In addition, proteolytic enzymes naturally found in plants are also being focused on by recent studies. At the molecular level, experiments to decrease PPO biosynthesis *in vivo* through antisense RNA method have also been undertaken (Martinez and Whitaker, 1995).

Despite the widespread role of PPO, there is limited understanding of its structure and interaction with various ligands. A deeper understanding on mechanisms by which PPO interacts with different molecules, especially inhibitors, is vital to fully utilize the enzyme in various applications. There are no strict structural requirements of a good PPO inhibitor *per se* but a similar trend is observed. Most inhibitors are either aromatic or sulfhydryl compounds, although for the latter a sulfo-quinone formation and not actual enzyme inhibition occurs (Ferrar and Walker, 1996). Hydroxyl groups are also implied in the inhibitory effect as they can undergo nucleophilic attack on the active site copper (Loizzo, Tundis, & Menichini, 2012). As expected, large, bulky substituents like phenyl groups, sugars, or long alkyl chains can cause steric hindrance, preventing the entry of substrate to the active site pocket, preventing PPO activity. The wide number and variety of enzymatic browning control methods show proof that this is an important area of concern especially for food producers. A great deal of researches are being undertaken to address the problem of food loss. However, considering all the determinants of food quality, it appears that no one perfect method to prevent undesirable browning can be pointed. Thus, it remains a challenge for food scientists to find the most effective method to curb the detrimental effects of PPO without sacrificing nutrition and food quality.

In this paper, the binding of inorganic inhibitor ligands, such as halides and disulfide, to PPO is studied. Particular notice is also placed on the effect of the redox transformations of the enzyme on the ligand binding. A detailed steady-state kinetic analysis of PPO activity and inhibition is likewise presented. NMR and electrochemical analyses of the PPO-ligand interaction are also described. Disulfide and halides were chosen as inhibitor ligands since they possess considerable redox character and their binding is assumed to occur directly to the copper center. These experiments aim to contribute to a further understanding of interaction of PPO with inorganic ligands. This knowledge is essential in developing better methods to control the destructive effects and to improve the beneficial uses of PPO.

This study was performed using commercially available tyrosinase isolated from the mushroom species *Agaricus bisporus* (EC 1.14.18.1). As this enzyme has been thoroughly characterized and shows high homology with mammalian tyrosinases, it is assumed that this enzyme is well suited as a model to study PPO activity and inhibition. Although mushroom PPO (mPPO) may be different with other PPOs in terms of amino acid sequence and over-all structure, it has been established that the active center of type-3 copper proteins is highly conserved across all organisms. Thus, it can be said that their active site structures and ability to bind molecular oxygen are constant regardless of the source. Likewise, it is assumed that kinetic and structural mechanisms proposed in this study can be generally applied to most organisms albeit with caution. Further, mushroom PPO is commercially available, at a lower cost, with a relatively higher purity as compared to enzymes extracted from plant sources.

Crystal structure of tyrosinase from Agaricus bisporus

A detailed description of the crystal structure of tyrosinase from the mushroom *Agaricus bisporus* was presented in a paper by Ismaya and collegues (Ismaya et al., 2011). As a thorough understanding of the PPO activity and inhibition mechanisms may be achieved with a knowledge of the crystal structure, this information from the published work of Ismaya and group will be presented here.

PPO is reported to be a tetrametric protein of 120 kDa size. It is assymetric, composed of two subunits of ~43 kDa size (H subunit) and two subunits with ~14 kDa size each (L subunit) (Figure 1.6). Each H-L dimer interaction is stabilized by polar and hydrophobic interactions. The L subunit adopts a lectin-like fold (Figure 1.7 B). However, its identity and function is yet to be understood. Electron density maps do not correspond to any of the C-terminal PPO sequences and a BLAST search against database did not result in any homologous proteins. In the activity assay, the specific activity of H_2L_2 form of mPPO was low as compared to the that of the H subunit alone. Further, the L subunit is also found located far away from the active site. From these observations, it was concluded that the L subunit is not essential for the activity of PPO. Nonetheless, it may have an involvement in the H subunit folding, Cu binding, or may contribute to the overall stability of the enzyme. Therefore, further studies on its function in tyrosinase is worth undertaking.

On the other hand, the core structure of the H subunit is similar to the other known tyrosinase domains, although containing about 100-120 residues more. It has in its structure 13 α-helices, eight short β-strands and many loops. The binuclear copper site, essential for catalytic activity, is found at the bottom of a spacious cavity in the surface of the H subunit, where the two ions are attached to the histidine residues in the helices α3, α4, α10, and α11 (Figure 1.7 A). CuA is bound to the N-ε of His61 (in α3), His85 (in the loop connecting α3 and α4), and His94 (in α4). CuB is liganded to His259, His 263(in α10) and His296(in α11) (Figure 1.7 A). The copper center is readily accessible from the solvent, free from occlusion by the L subunit or by side chain loops (Ismaya et al., 2011).

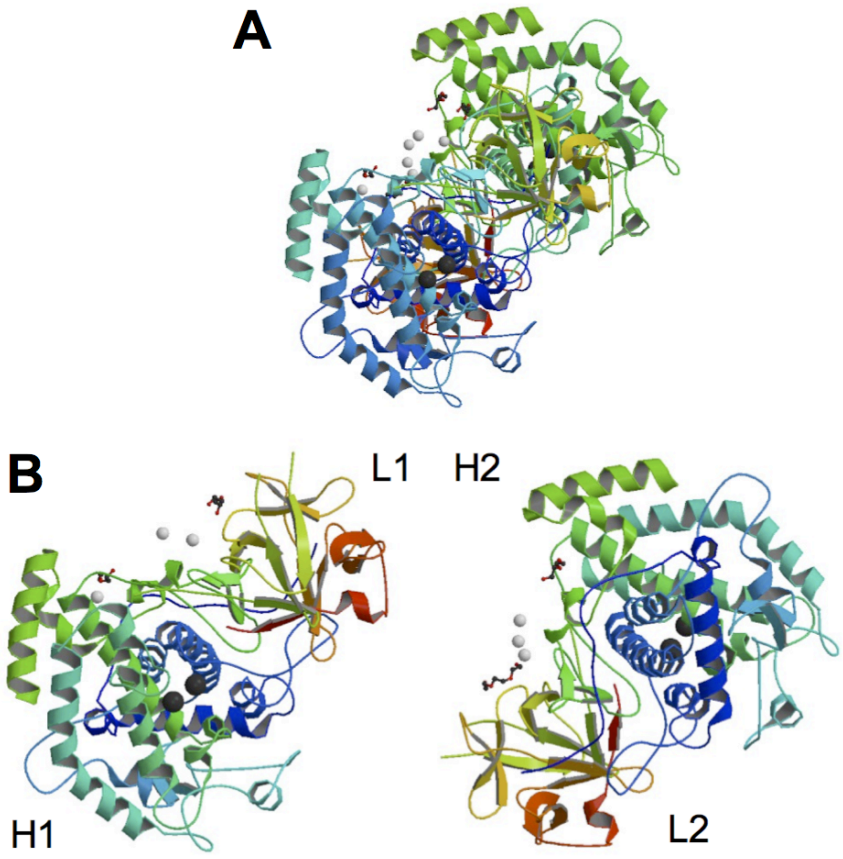

Figure 1.6 Structure of *A.bisporus* tyrosinase.

(A) Cartoon representation of the *A. bisporus* tyrosinase H_2L_2 tetramer structure. (B) Individual dimer units of H1-L1 and H2-L2. The black spheres embedded in the H units indicate the copper ions. The figures were obtained from the Protein Data Bank with accession code 2Y9W.

Figure 1.7 Cartoon representation of the individual subunits in *A.bisporus* tyrosinase.
(A) The H unit, including the binuclear copper center (orange spheres). The α-helices containing the six copper-coordinating histidine residues are indicated. (B) the L subunit. The following figures are from the published work of Ismaya et al. (2011).

Chapter 2 Kinetic Analysis of PPO Activity and Inhibition by Halides[1]

In the presence of molecular oxygen, PPO catalyzes the ortho-hydroxylation of phenolic compounds and can further oxidize the diphenols to form the corresponding quinones. Because of the detrimental effects of PPO oxidation on food, the control of PPO activity is an on-going study of interest. Various compounds have been proposed for use as PPO inhibitor and it was observed that the mechanism of inhibition of PPO varies according to the structure and chemistry of the inhibitor ligand. Sodium chloride is a biologically significant salt, readily available and found in most biological systems. In this chapter, the inhibition of halides on mushroom tyrosinase, henceforth referred to as mPPO, was described by a steady-state kinetic analysis. Non-competitive, and uncompetitive inhibition mechanism were observed on mPPO, depending on the inhibitor used. Substrate inhibition was also observed at high catechol concentrations and it also showed effect on the degree of halide inhibition. At high catechol concentration, the inhibition effect of halides is decreased. Likewise, substrate inhibition was abated when high concentrations of halides are added. The results led this study to propose that halides and excess substrate compete for affinity to an allosteric site in mPPO.

I. Materials and Methods

The commercially available tyrosinase isolated from *Agaricus bisporus* species of mushroom (EC 1.14.18.1) which was used as the PPO source, and catechol were purchased from Sigma-Aldrich (St. Louis, MO, USA). The halide salts sodium chloride (NaCl), sodium bromide (NaBr), and sodium iodide (NaI) were procured from Kokusan Chemical (Kanagawa, Japan), Kanto Chemical (Tokyo, Japan), and Nacalai Tesque (Kyoto, Japan) respectively. All reagents are of analytical grade and used as is without further purification.

Enzyme Activity Assay

Polyphenol oxidase activity was determined based on the conversion rate of catechol to o-quinone, monitored by an increase in the absorbance at 410 nm, following the method of Unal (2007). At this wavelength, maximum absorbance of the quinone products is observed. After 2,650 μL of buffer (0.2 M acetate buffer, pH 5.0) was placed in a quartz cell (optical length of 1 cm), 300 μL catechol was added. The solution was equilibrated with constant

[1] The results in this chapter have been previously presented in the masters thesis of the same author.

stirring at 30°C using an ETC-505T temperature controller (JASCO, Tokyo, Japan). Upon stabilization at the required temperature, 50 µL of PPO solution (final concentration, 2 µg/mL) was added to initiate the reaction. Using a JASCO V-55 UV-Vis spectrophotometer, the absorbance of the resulting solution was read at 410 nm for 15 s, during which time the absorbance increased linearly. The enzyme activity is defined as the amount of enzyme that converts 1µmol of substrate per minute, at the conditions of the assay (molar absorptivity coefficient is estimated at 1417 M^{-} cm^{-}) (Raynova, et al., 2014). The final catechol concentration was varied (0.05, 0.1, 0.2, 0.4, 0.8, 1.0, 2.0, 3.0, 4.0, 5.0, and 100.0 mM) to see the change in the reaction at different substrate concentrations.

Inhibition of mPPO activity by halides

The same method as for activity assay was followed but halide at final concentrations of 0, 0.5, 5.0, and 10.0 mM were included to understand the effect of halide concentration. All of the above tests were performed with NaF, NaCl, NaBr, and NaI. All assays were performed in triplicate with the result expressed as the mean ± standard deviation, and the assays were repeated.

pH dependence of inhibition

The buffer was varied to see the effect of pH on enzyme activity and inhibition. Unless specified otherwise, acetate buffer was used for assays done at pH 5.0 and 5.5, phosphate buffer for pH 6.0 and 6.5, while HEPES was used for pH 7.0 and 8.0.

Nonlinear regression

Nonlinear least-squares analysis was performed using OriginPro 8.6 (Origin Lab, Northhampton, MA, USA).

II. Results

Effect of pH on mPPO activity

The activity of mPPO was observed in different pH conditions (Figure 2.1). The activity of mPPO did not vary even with changing pH at the lower range for both catechol concentrations. However, around a 50% increase at neutral pH was observed when 5 mM catechol was used. At 1 mM catechol, activity increased but with a lesser degree. At pH 8.0, high absorbance value was observed even prior to the addition of the enzyme, suggesting the auto-oxidation of the substrate in basic pH. This seems logical because a more pronounced high activity is seen in 5 mM catechol, but not so much in 1 mM catechol. Therefore, the increase in absorbance at pH 8.0 cannot be attributed to activity, rather, to auto-oxidation. This capability of catechol to react with molecular oxygen without enzymatic assistance in alkaline conditions was also mentioned in a review paper by Rescigno et al. (2002). Disregarding the results for pH 8.0, because of autooxidation in basic conditions, PPO showed the highest activity at pH 7.0 for both catechol concentrations. This is in agreement with optimum pH value for mushroom PPO reported elsewhere (Oz et al., 2013; Inamdar, Joshi, & Jadhav, 2014).

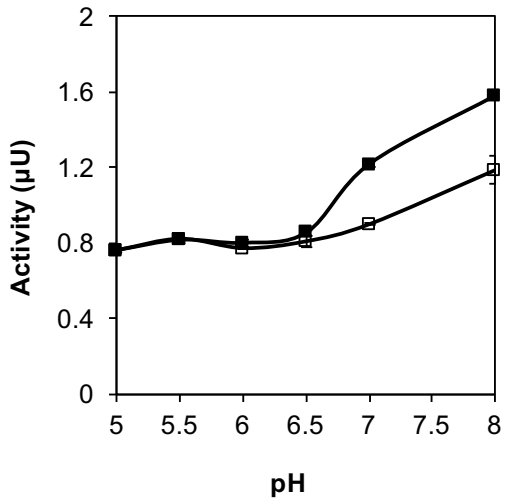

Figure 2.1 mPPO activity under different pH conditions.
mPPO activity was measured by monitoring the increase of absorbance at 410 nm under different pH conditions. 1 mM (white squares) and 5 mM (black squares) catechol were used as substrate.

Estimation of Km and Vmax

Following the mPPO-catalyzed oxidation of 1 mM catechol, the plot of absorbance versus time shows a steady increase in activity over time, until a maximum point when curve

reaches a plateau, indicative that PPO obeys Michaelis-Menten kinetics in all pH levels tested (Figure 2.2).

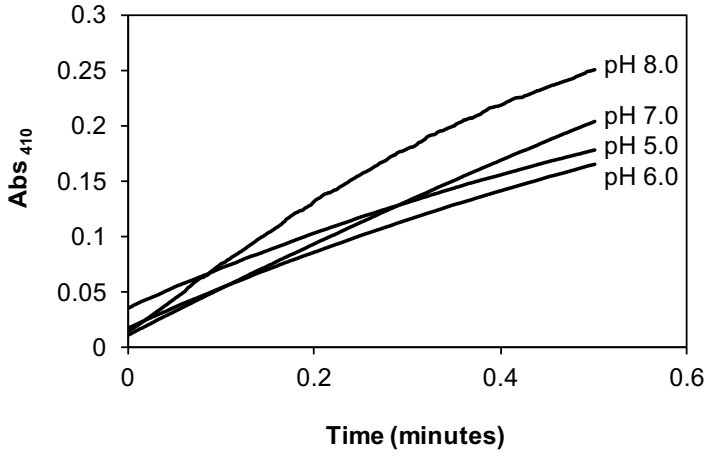

Figure 2.2 Time-course plot of catechol oxidation in varying pH.
Absorbance increased hyperbolically with time, suggesting that PPO follows Michaelis-Menten kinetics.

The kinetic constants, *Km* and *Vmax*, of PPO were estimated from linearized Lineweaver-Burke (Figure 2.4 A) and Hanes plots (Figure 2.4 B) using data of PPO activity versus catechol concentration at pH 5.0, or at the pH level used throughout this study (Figure 2.3).

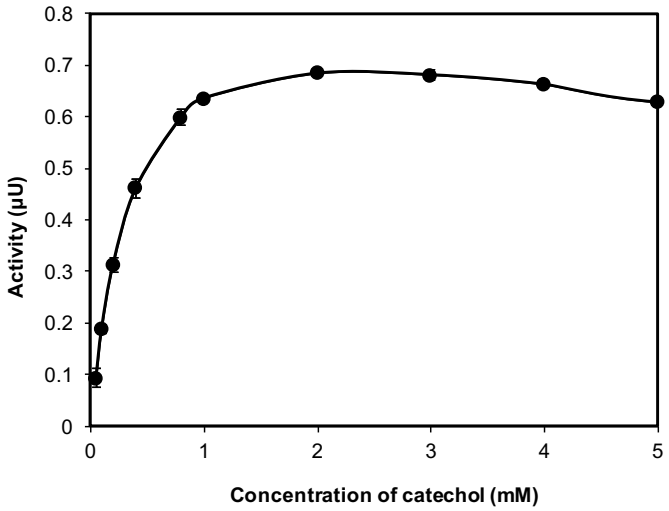

Figure 2.3 Rate of catechol oxidation as a function of concentration
The assay was carried out at 30°C and at pH 5.0, where inhibition was most evident. Enzyme activity increased with catechol concentration, characteristic of a Michaelis-Menten kinetic mechanism. The final concentration of PPO was 2 µg/ mL.

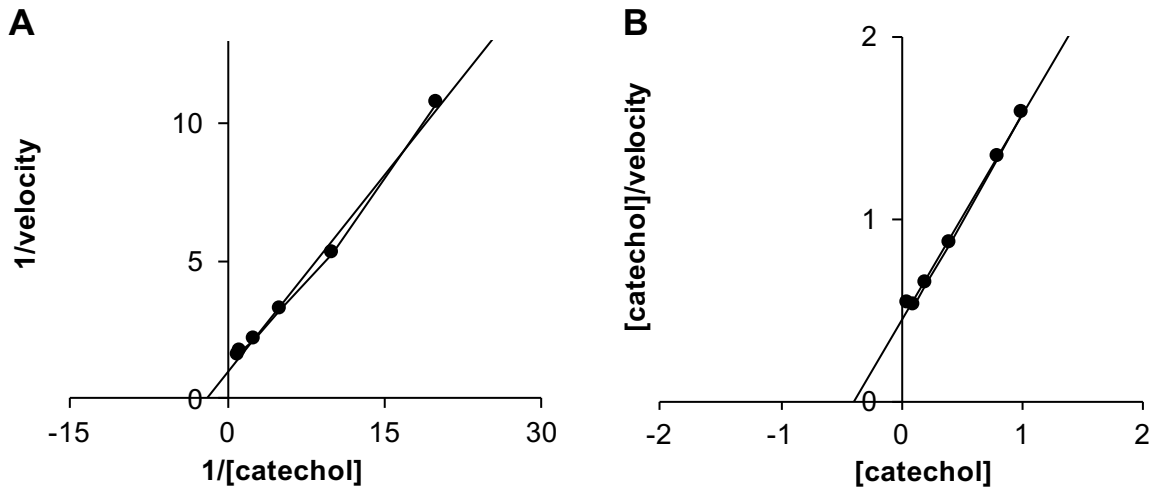

Figure 2. 4 Estimation of kinetic parameters from reciprocal plot**.**
Lineweaver- Burke (A) and Hanes (B) plot were drawn to estimate the kinetic constants. Data points are taken from empirical data in Figure 2.3.

Both plots exhibit linear trend, representative of a Michaelis- Menten mechanism. From both plots, *Km* and *Vmax* values are estimated at 0.4 mM and 0.95 μU respectively. The results of the linearized plots are in close agreement with the values from the regression analysis (Table 2.1).

Table 2.1 Estimate of mPPO kinetic parameters based from the enzyme activity as a function of catechol concentration

V_{max} (μ U)	K_m (mM)
0.87 $\pm$ 0.01	0.36 $\pm$ 0.01

Inhibition by halides

mPPO activity was measured with the inclusion of NaF, NaCl, NaBr, and NaI as halide inhibitors in pH 5.0 (Figure 2.5 A) and 7.0 (Figure 2.5 B). mPPO-catalyzed oxidation of 1 mM catechol was monitored by the increase in absorbance at 410 nm in the presence and absence of the halide inhibitors. In pH 5.0, mPPO activity was decreased by the sodium halides in a dose-dependent manner, although the inhibition slightly decreased at higher concentration (Figure 2.5 A). However, when the enzyme activity was measured at neutral pH, the inhibition effect of halides was evident only at high concentration of inhibitor (Figure 2.5 B).

To get the optimum pH level for succeeding halide inhibition experiments, the same experiment in Figure 2.5 was repeated, using six different pH conditions. Results are shown in Figure 2.6.

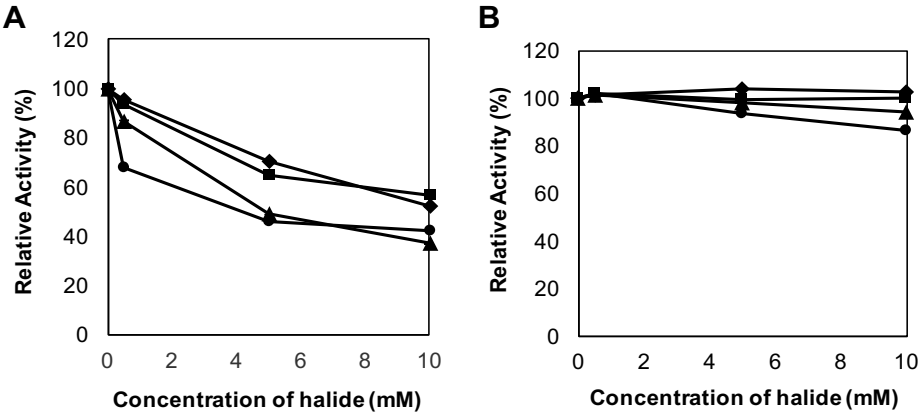

Figure 2.5 PPO oxidation in the presence of halides in pH 5.0 and 7.0.
PPO was assayed with 1 mM catechol in the presence of 0, 0.5, 5.0, and 10.0 mM NaF (black circles), NaCl (black diamonds), NaBr (black squares), and NaI (black triangles) at pH 5.0 (A) and pH 7.0 (B).

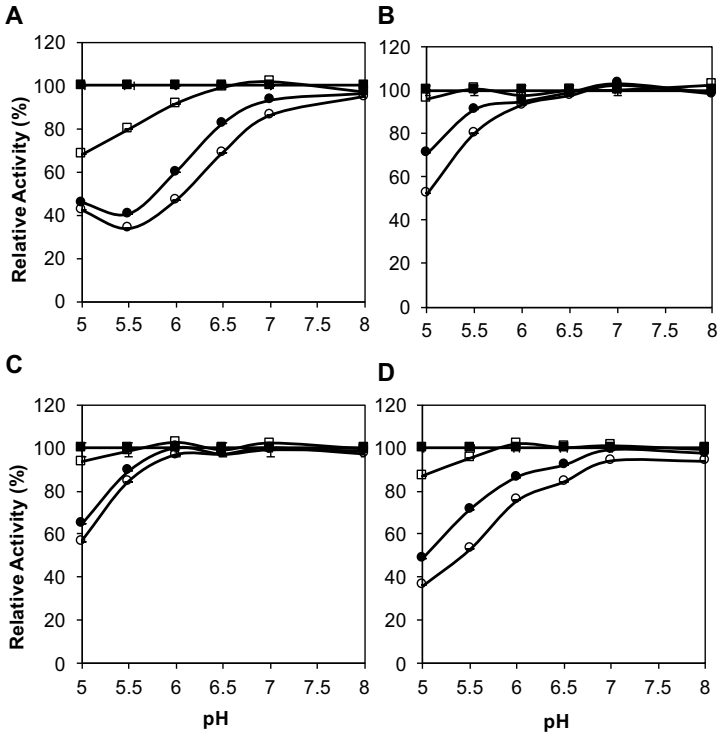

Figure 2.6 The effect of pH on halide inhibition.
PPO activity was assayed in the presence of NaF (A), NaCl (B), NaBr (C), and NaI (D) inhibitors in different pH conditions. Concentrations of halides are 0 mM (black squares), 0.5 mM (white squares), 5 mM (black circles), and 10 mM (white circles). All succeeding assays with halides were performed at the pH where inhibition was most evident.

From among all pH conditions tested, inhibition was most evident at pH 5.0 and 5.5. In these acidic conditions, PPO activity decreased with increasing halide concentration. At near-neutral to slightly basic pH, the behavior varies with the type of halide. For fluoride and iodide (Figures 2.6 A and D, respectively), inhibition effect decreased as pH was increased. In contrast, almost no change in activity was observed at near-neutral to slightly basic pH for chloride and bromide (Figures 2.6 B and C, respectively). At pH 6.5 to 8.0, the activity of the uninhibited PPO did not vary much compared with the solution containing 10 mM sodium bromide and sodium chloride. From the results, it can be observed that fluoride and iodide binding to mPPO is strongly influenced by pH. In this case, two possible binding sites are considerable. First, fluoride or iodide binds to ionizable groups in mPPO. It could also be considered that binding of fluoride or iodide is influenced by the oxidation state of copper in the active site, as this is also influenced by the pH. Chloride and bromide show an almost identical kinetic behavior, both showing intermediate behavior in terms of pH effect (Figure 2.6 B and C).

Figure 2.7 shows that the inhibition was not due to the sodium ion as the relative activity of PPO did not change even when Na_2SO_4, of equivalent ionic strengths, were used instead of the sodium halides as inhibitors in the assay solution.

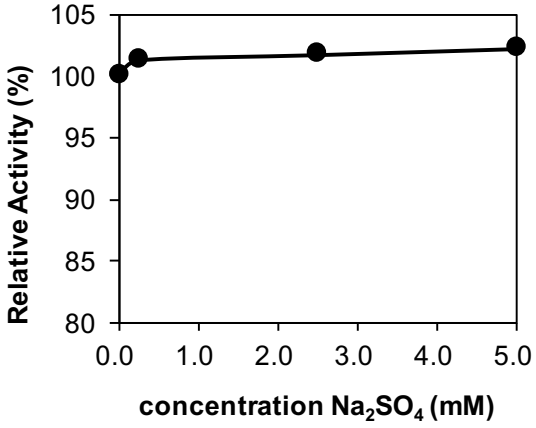

Figure 2.7 PPO activity in high ionic strength.

Na_2SO_4 of equivalent ionic strengths were substituted for halides and the enzyme was assayed using the same conditions. The relative activity did not change compared to the control, even with a high concentration of Na_2SO_4. It can be presumed that the inhibition was caused by halides and not from the sodium ion.

The experiment was repeated, using different concentrations of the substrate (Figure 2.8). The slope of the curve became smaller with increasing chloride and bromide concentration, but activity was not totally eliminated even at the highest concentration of inhibitor tested. In contrast, almost complete inactivation occurred for fluoride concentration more than 0.5 mM. Iodide also showed strong inhibition even at low concentration.

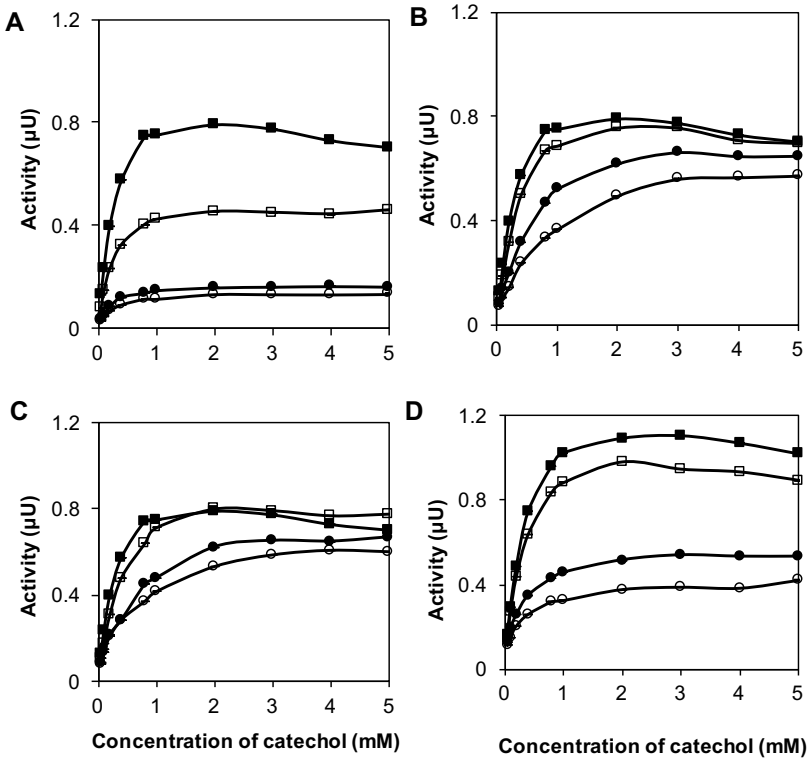

Figure 2.8 PPO activity and halide inhibition as a function of catechol concentration.
Polyphenol oxidase (PPO) activity plotted as a function of catechol concentration in the presence of NaF (A), NaCl (B), NaBr (C), and NaI (D). The halide concentrations are 0 (black squares), 0.5 (white squares), 5.0 (black circles), and 10.0 mM (white circles).

Lineweaver- Burke plots were drawn using data at pH 5.0 from Figure 2.8 to characterize the type of inhibition (Figure 2.9). The Michaelis constant was estimated from the plots and was also estimated by nonlinear regression analysis.

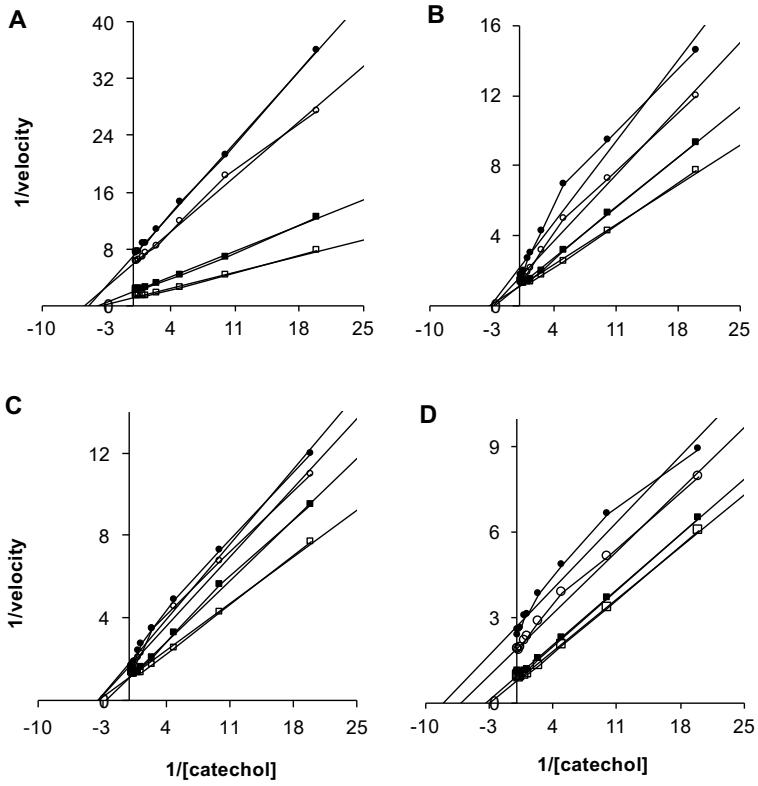

Figure 2.9 Double reciprocal plot to determine mechanism of halide inhibition.
Double reciprocal plot for the inhibition of mPPO by NaF (A), NaCl (B), NaBr (C), and NaI (D) at pH 5.0. K_m values were estimated from data points taken from empirical data in Figure 2.8. The graphs of fluoride (K_m= 0.2 mM), chloride (K_m= 0.33 mM), and bromide (K_m=0.25 mM) show non-competitive behavior. The plots of iodide inhibition show parallel K_m and Vmax changes, characteristic of uncompetitive inhibition.

In the double reciprocal plots of fluoride, chloride, and bromide, the slope decreased with increasing inhibitor concentration, indicating a change in Vmax. However, all lines again converged at a similar point. Therefore, the K_m of the enzyme did not change, even with the addition of inhibitor. Such characteristic show that fluoride, chloride, and bromide inhibit mPPO via a non-competitive mechanism. In this type of inhibition, the halide binds to either the enzyme or the enzyme-substrate complex.

On the other hand, the plots of iodide inhibition showed parallel plots with changing inhibitor concentration. Both K_m and Vmax values are changed, indicative of an uncompetitive inhibition. In uncompetitive inhibition, it is assumed that iodide binds only to the enzyme-substrate complex. The binding to the free enzyme is thought to be weak, and the bound substrate helps the inhibitor in binding.

Substrate Inhibition in mPPO

Substrate inhibition was observed when high concentrations of catechol were used in the assay, as seen in Figure 2.10. At substrate levels lower than 1 mM, PPO activity obeyed Michaelis-Menten kinetics, with enzyme activity increasing with substrate concentration until it reached highest velocity (Figure 2.10 inset). In contrast, at catechol concentrations greater than 1 mM, increasing concentrations of catechol reduced PPO activity. This is indicative of substrate inhibition where inhibition effect overweighed the velocity increase.

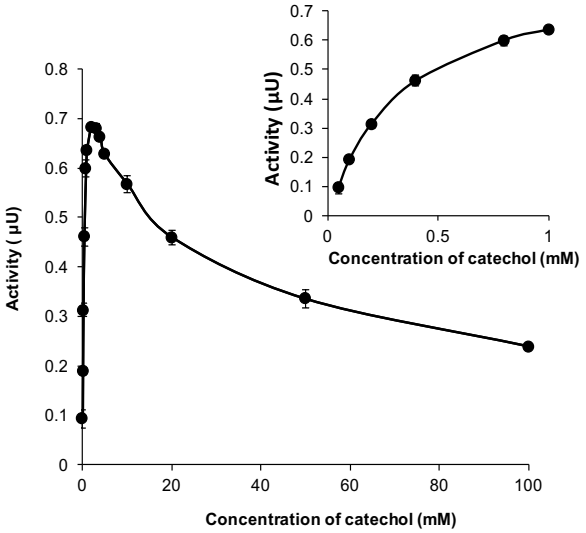

Figure 2.10 Substrate inhibition in mushroom PPO.
Mushroom polyphenol oxidase (mPPO) activity was plotted as a function of catechol concentration. The assay was carried out at pH 5.0 and 30°C. Activity increased with catechol concentrations up to 1 mM, after which it decreased and then reached an almost plateau value at 100 mM catechol. The expanded figure of catechol concentrations from 0.05 to 1.0 mM is displayed in the inset.

The experiment was extended to a concentration of 50 mM catechol (Figure 2.11). As expected, a decreased activity was seen at all pH values, confirming substrate inhibition. Similar to halide inhibition, the biggest decrease in activity caused by excess substrate is observed at acidic pH values. At pH 7.0, the activity was very similar with the uninhibited enzyme. An enhanced activity at the optimum pH is again assumed, and in this situation, inhibition effect was overruled by high enzyme activity. No explanation can be given for the sharp drop in PPO activity using 50 mM catechol at pH 8.0, except for artefact.

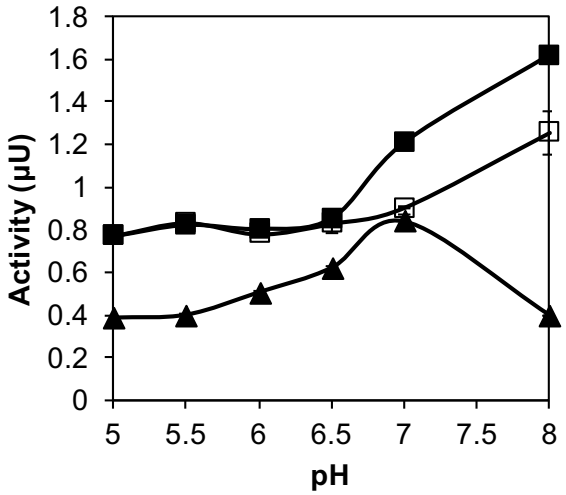

Figure 2.11 pH effect on substrate inhibition.

PPO activity was assayed in different pH conditions to observe its effect on substrate inhibition. The catechol concentrations were 1 mM (white squares) and 5 mM (black squares). Data was also taken for PPO activity when catechol concentration is 50 mM (black triangles), where substrate inhibition may be assumed.

Substrate and Halide Inhibition in PPO

Another interesting phenomenon can be observed from the data in Figure 2.8. It is seen that the halides decreased PPO activity in a dose-dependent manner. However, the degree to which the halide inhibited the reaction was dependent on the substrate concentration; the most prominent inhibition was found at catechol concentrations below 2 mM, after which an increased concentration gradually lowered the degree of inhibition. This finding indicates that substrate inhibition was reduced with an increase in halide concentration. To validate this observation, a much higher concentration of catechol (100 mM) was used (Figure 2.12). At this concentration, no apparent halide inhibition was evident in NaCl, NaBr, and NaI and the enzyme activity at various halide concentrations almost converged to a similar value. Thus, high concentrations of catechol induced severe substrate inhibition and concurrently diminished the inhibition by halide. In contrast, 10 mM NaF showed very strong inhibition. At 100 mM catechol, the remaining activity was ten-fold less than for the other halides. Because of the significant deviation of fluoride, it is assumed that its inhibition on PPO activity follows a separate mechanism that remains unclear at this point.

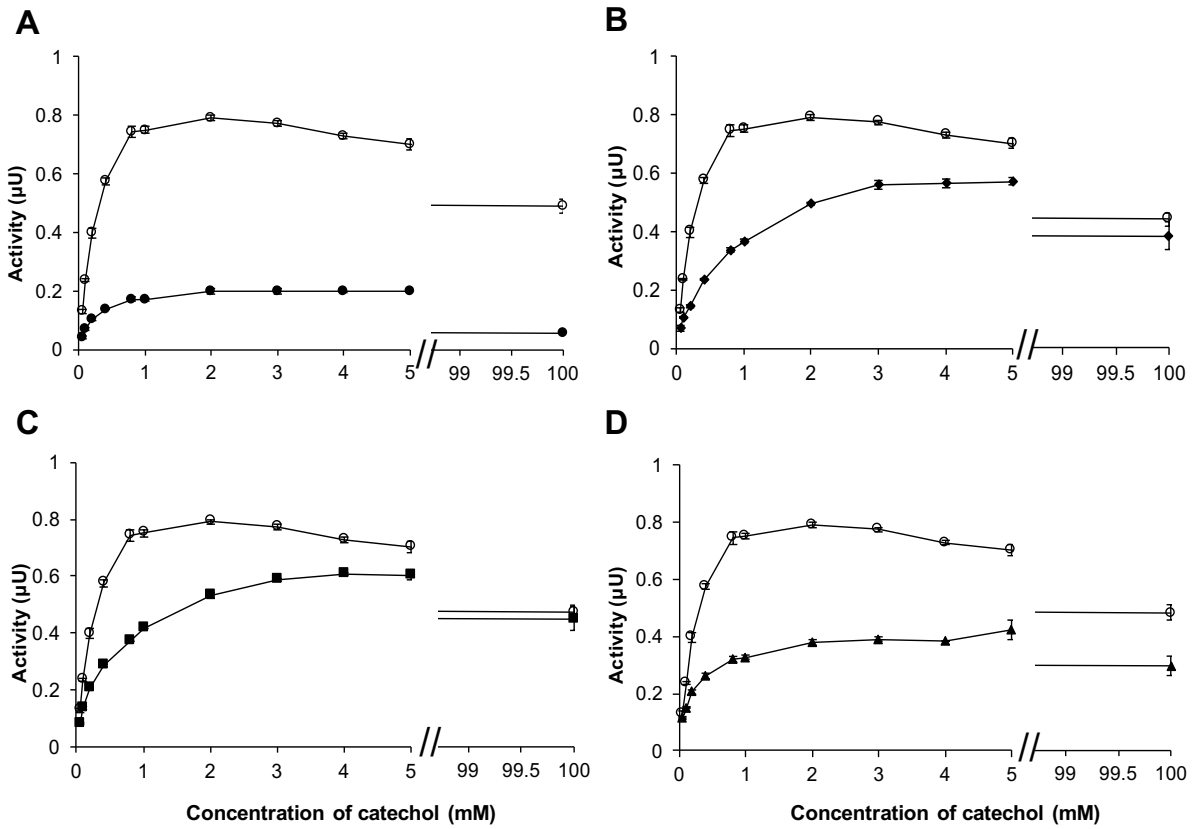

Figure 2.12 Halide inhibition at high catechol concentration.

The inhibition of halides is decreased by high concentrations of catechol and vice versa. At 100 mM catechol, inhibition of halide is diminished, especially for 10 mM NaCl (B) and 10 mM NaBr (C), where the enzyme activity of the uninhibited (white circle) and inhibited mPPO (black diamonds and black squares, respectively) converged to a similar point. mPPO inhibition by 10 mM NaI (D, black triangles) was also decreased by high catechol concentration. 10 mM NaF (A) showed very strong inhibition even at low concentration. The following assay was performed at pH 5.0.

III. Discussion

Substrate and Halide Inhibition of mushroom PPO

Substrate inhibition was observed when mushroom PPO was assayed in high concentration of catechol at pH 5.0. This phenomenon was previously reported for L-DOPA oxidation by fungal PPO where the activity of partially-purified *Lentinula boryana* decreased at L-DOPA concentrations greater than 10 mM (De Faria et al., 2007). In bean PPO, inhibition already occurred at 25, 15, 75, and 10 mM concentrations of catechol, 4-methylcatechol, pyrogallol, and L-DOPA, respectively (Paul and Gowda, 2000). Rojo, Gomez, and Estrada mentioned of substrate inhibition of mushroom tyrosinase by 4-methylcatechol at greater than 1 mM at pH 6.5 (Rojo, Gomez, & Estrada, 2001). In substrate inhibition, it can be imagined that the first substrate molecule binds to the mPPO active site in a normal manner then a second substrate molecule will bind to a second inhibitory site. In principle, this is a type of uncompetitive inhibition, where the inhibitor (in this case, the surplus substrate) binds to an allosteric inhibitory site. In low catechol concentration, the catalytic function dominates. However, at higher substrate concentration, the inhibitory function prevails.

The substrate inhibition that occurs in mPPO suggests that mushroom PPO possesses two catechol-binding sites: the active site (Site A) and the other is an allosteric inhibitory site (Site B). The following scheme (Scheme 1) illustrates substrate inhibition in PPO:

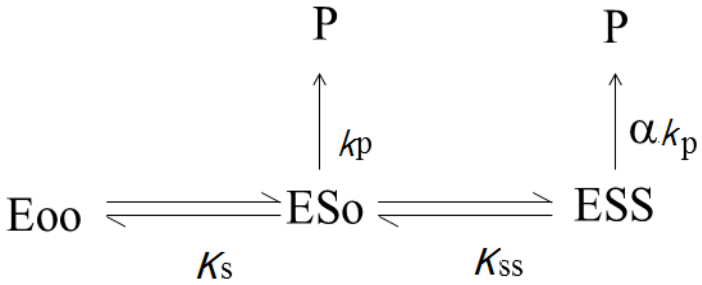

Scheme 1 Reaction scheme for substrate inhibition of polyphenol oxidase (PPO). EXY denotes a PPO molecule occupied by X and Y at the first (site A) and the second (site B) catechol-binding site, respectively, where S indicates substrate and o represents an unoccupied site. K_s and K_{ss} denote dissociation constants, which are expressed as K_s = [Eoo][S]/[ESo] and K_{ss} = [ESo][S]/[ESS]. k_p is a turnover number for the product formation from ESo complex and α is a ratio relative to the turnover number for the reaction from ESo to Eoo and P.

From this reaction scheme, using the catechol concentration [S], the reaction velocity, *v*, can be estimated as follows:

$$v = \frac{V_{max} \cdot [S] \cdot (1 + \alpha \frac{[S]}{K_{ss}})}{K_s + [S] \cdot (1 + \frac{[S]}{K_{ss}})} \qquad \text{(Equation 2.1)}$$

In Equation 2.1, *Ks* and *Kss* denote dissociation constants of the following reactions respectively:

ESo ↔ Eoo + S,

ESS ↔ ESo + S,

Where S is the catechol substrate while V_{max} is the maximum reaction velocity, which corresponds to the product of the turnover number, *kp* (Scheme 1), for product formation from the ESo complex and the concentration of PPO. In addition, α is the ratio of the turnover number for product formation from the ESS complex to that for product formation from the ESo complex.

A nonlinear least-squares analysis undertaken for the data set shown in Figure 2.10 yielded the results presented in Table 2.2. The parameters seem to be consistent because the simulated curve agrees with the activity obtained experimentally. The α value given in Table 2.2 reveals that mushroom PPO with catechol at site B retained as much as 20% of the activity of the unoccupied enzyme.

Table 2.2 Estimation of the polyphenol oxidase (PPO) substrate inhibition parameters determined from the enzyme activity as a function of the catechol concentration

V_{max} (μU)[b]	K_s (mM)[b]	K_{ss} (mM)[b]	α [b]	R^2 [c]
0.87 ± 0.34	0.35 ± 0.05	14.82 ± 0.75	0.19 ± 0.01	0.998

[a] Figures represent the estimated value ± standard error (n = 3)

[b] The parameters V_{max}, K_s, K_{ss}, and α are defined in the text

[c] R is the correlation coefficient between the estimated activity and that determined experimentally

Halide inhibition was also experienced by mPPO when tested against various concentrations of the halide. From the results shown in Figure 2.5, it is evident that halide inhibits PPO in a dose-dependent manner. At pH 5.0, inhibition by halides follow the order $F^- > I^- > Cl^- = Br^-$. At

the highest concentration of fluoride tested, less than 20% activity of the uninhibited enzyme was retained. Iodide showed likewise showed strong inhibition at pH 5.0, albeit less strong than fluoride. Chloride and bromide showed similar intermediate inhibitory behavior. The order of inhibition gives clue that the ionic size may also be contributory to the effectiveness of the halide. Fluoride, being the smallest ion, has the highest accessibility to the active site, forming a very stable binding to the copper at the mPPO active site. An almost similar pattern of behavior was reported by the group of Martinez when they measured halide inhibition on mushroom PPO using L-DOPA at pH 6.5. In their paper, they mentioned that the extent of halide inhibition is dictated by either of two factors: 1) the halide ionic size, which affects its accessibility to the enzyme active site, and 2) strength of interaction of the ion with copper. They postulated that, in mushroom tyrosinase, the reason for the order of halide inhibition was a combination of both factors (Martinez et al., 1986).

A double reciprocal plot of different concentrations of halides were drawn to characterize the mode of inhibition. In this plot, chloride and bromide show strikingly similar behavior. Here, the lines differ in the slope and did not converge at the ordinate axis. Rather, the common intersection point is located at the left of the y-axis. In this inhibition, Vmax changes while the *Km* value remains unchanged. Further, halide binding is possible for both free enzyme and the enzyme-substrate (ES) complex. In the case that both substrate and inhibitor binds to mPPO, it is understood that both compounds influence each other in binding to the protein. Considering the scheme of halide inhibition in mPPO (Scheme 2), the relative affinity of halides to the free or the ES complex is described by the inhibition constants Kh_1 or Kh_2, respectively.

Iodide shows a different behavior of inhibition. In the Lineweaver-Burke plot, all lines are parallel with each other with no common intersection point. Vmax and *Km* changes with the change in halide concentration. This is representative of uncompetitive inhibition, where the iodide inhibitor binds exclusively to the enzyme-substrate complex. Binding of iodide to mPPO is described solely by Kh_2.

Because of the very strong inhibition exhibited by fluoride even at low concentrations, the proposed scheme cannot be readily assumed for this halide. It is commonly encountered that fluoride follows a different chemistry that its related halides. Moreover, fluoride can behave as a weak acid, further complicating its mechanism. Because of its small ionic size, the

negative-charged valence electrons are concentrated closer to the nucleus where they repel each other. Thus, fluoride is difficult to ionize and F^- species are unstable. This causes the behavior to be different from the other halides. The exact kinetic mechanism of fluoride deserves a deeper study, which is beyond the scope of this paper.

The following scheme describes halide inhibition in mushroom polyphenol oxidase:

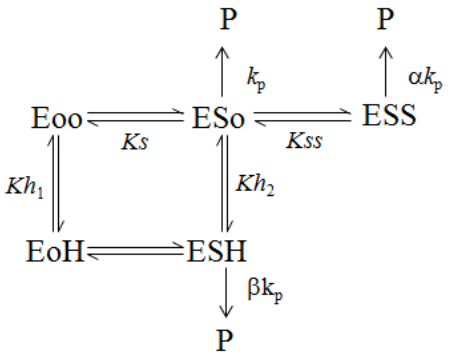

Scheme 2 Scheme of halide inhibition of mushroom polyphenol oxidase (mPPO). Nomenclature is same as that used in Scheme 1. In this scheme, H denotes halide. K_{h1} and K_{h2} indicate dissociation constants, which are expressed as K_{h1} = [Eoo][H]/[EoH] and K_{h2}= [ESo][H]/[ESH]. β is the ratio relative to the turnover number for the reaction from ESo to Eoo and P.

and the following equation is used to estimate the reaction velocity:

$$v = \frac{V_{\max} \cdot [S] \cdot (1 + \alpha \frac{[S]}{K_{ss}} + \beta \frac{[H]}{K_{h2}})}{K_s \cdot (1 + \frac{[H]}{K_{h1}}) + [S] \cdot (1 + \frac{[S]}{K_{ss}} + \frac{[H]}{K_{h2}})} \qquad \text{(Equation 2.2)}$$

Following the scheme in Scheme 2, K_{h1} and K_{h2} are the respective dissociation constants of the following equations:

EoH ↔ Eoo + H (for binding to the free enzyme)

ESH ↔ ESo + H (for binding to the enzyme-substrate complex)

All other nomenclature follows that used in the previous equations.

The results of the kinetic experiment show that both substrate and halide inhibition occurs for mushroom PPO at pH 5.0. In both cases, the binding is assumed to occur at an allosteric site,

which we assigned as Site B (Figure 2.13). Moreover, it appears that excess substrate and halide compete with each other for binding at Site B.

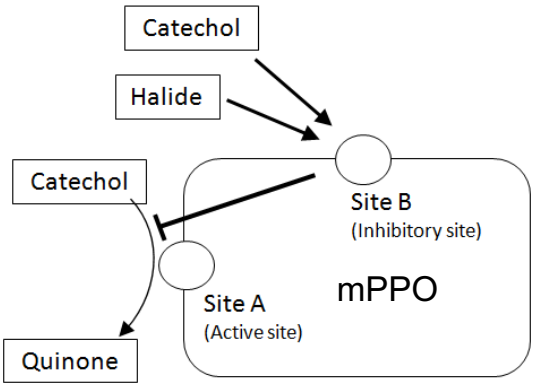

Figure 2.13 Illustration of the catechol reaction model and halide inhibition of mushroom PPO. Catechol and halides compete with each other for binding to Site B, both of which inhibit the oxidase activity of mPPO.

Table 2.3 Estimation of the mushroom polyphenol oxidase (mPPO) parameters for halide and substrate inhibition determined from the enzyme activity as a function of catechol concentration[a]

	V_{max} (μU)[b]	K_s (mM)[b]	K_{ss} (mM)[b]	α [b]
NaCl	6.07 ± 0.20	0.37 ± 0.03	6.20 ± 0.87	0.27 ± 0.01
NaBr	8.48 ± 0.34	0.43 ± 0.04	8.82 ± 1.79	0.24 ± 0.02
NaI	8.54 ± 0.19	0.43 ± 0.02	7.42 ± 0.73	0.25 ± 0.01

	K_{h1} (mM)[b]	K_{h2} (mM)[b]	β [b]	R^2 [c]
NaCl	3.20 ± 0.46	23.46 ± 13.27	0.23 ± 0.21	0.996
NaBr	2.34 ± 0.42	4.40± 1.14	0.52 ± 0.03	0.996
NaI	5.34 ± 0.70	1.97 ± 0.14	0.13 ± 0.01	0.999

[a] Figures represent estimated value ± standard error (n = 3)
[b] The parameters V_{max}, K_s, K_{ss}, α, K_{h1}, K_{h2}, and β are defined in the text
[c] R is the correlation coefficient between the estimated activity and that determined experimentally

The kinetic constants provided in Table 2.3 describe, in detail, the halide binding and its corresponding effect on substrate affinity to mPPO.

a. Binding of halide and catechol to Site A (Ks vs. Kh_1)

Both halide and catechol can bind to Site A, the binding of which is characterized by Kh_1 for halide and *Ks* for catechol. Kh_1 values of chloride, bromide, and iodide are greater than the dissociation constant of catechol, indicative of a weaker binding to the free enzyme. Thus, at low catechol concentration where its catalytic function predominates, the substrate preferentially binds to Site A more than the halide.

In the case that the situation is reversed, wherein halide first binds to the free enzyme, the dissociation constant (K_{sh}) of the reaction ESH $\leftrightarrow$ EoH + S can be calculated from K_s, K_{h1}, and K_{h2} values. The results are tabulated in Table 2.4. A comparison between K_{sh} and K_s values for the respective halides showed that the binding of chloride and bromide will reduce the affinity of catechol to site A. The effect is greater with chloride than with bromide. Iodide has the opposite effect. These modulations of affinity strongly suggest that the structure of site A can altered upon the binding of halide to site B and that a change in the structure can cause the inhibitory effect. Furthermore, binding of halide to site B appear to significantly modulate the affinity of catechol to site A.

Table 2.4 Calculated dissociation constants, K_{sh} from the estimated parameters in Table 2.2

K_{sh} (mM)		
NaCl	NaBr	NaI
2.71 ± 1.60	0.81 ± 0.27	0.16 ± 0.02

Figures represent estimated value ± standard error.

b. Binding of halide to Site A or Site B (Kh_1 vs. Kh_2)

Comparison of the dissociation constants Kh_1 and Kh_2 explains the affinity of halide to either the free or the ES complex (Table 2.3). For bromide and chloride, Kh_1 has a smaller value than Kh_2, showing higher affinity to the free enzyme. The difference in affinity is more pronounced for chloride than in bromide. At this point, this difference in the ionic size may have an effect on the degree of affinity. In iodide reaction, the dissociation constant for binding to the free enzyme is greater. Thus, a stronger affinity to the ES complex is expected. This could explain the different behavior of iodide in the Lineweaver-Burke plot. Moreover, this result partially supports the assumption of an uncompetitive inhibition mechanism by iodide.

c. Effect of halide binding to surplus substrate binding to Site B

Kss describes the strength of affinity of excess substrate to the allosteric site. The results in Table 2.3 shows that *Kss* was decreased in the presence of halides, as compared to the uninhibited mPPO. This shows that the binding of halide to Site A affects the binding of excess catechol to site B.

Our findings unambiguously demonstrate that halides inhibit mushroom PPO activity by binding to an allosteric site we assigned as Site B. An allosteric interaction is evident, wherein the binding of halide might possibly cause a conformational change in the protein, preventing the binding of the catechol substrate.

However, it cannot be neglected that other mechanisms have been proposed for the halide inhibition of PPO activity. These discrepancies may result from different experimental conditions or from the different source of PPO used. Noncompetitive inhibition was observed for apple PPO, in which 4-methylcatechol was used as the substrate, and the reaction was conducted at pH 4.5 (Janovitz Klapp et al., 1990). This suggests a difference in enzyme properties between apple and mushroom PPO. Park and colleagues proposed an uncompetitive mechanism for the inhibition of mushroom PPO by chloride, in which L-DOPA is used as the substrate and the enzyme reaction proceeds at a pH of 7.0 (Park et al., 2005). In addition, higher levels of NaCl (0-120 mM) were used in those experiments. Therefore, the phenomena observed on our experiments may differ from those reported by Park and coworkers.

Alternatively, the proposed enzyme reaction scheme may still be in part valid for the other cases of chloride inhibition. Under the conditions that substrate concentration is much lower, the term [S]/K_{ss} may be neglected and Eq. (2.2) can be deduced to

$$v = \frac{V_{\max} \cdot [S] \cdot (1 + \beta \frac{[H]}{K_{h2}})}{K_s \cdot (1 + \frac{[H]}{K_{h1}}) + [S] \cdot (1 + \frac{[H]}{K_{h2}})}$$

Therefore, the abscissa intercept, 1/[S], of the Lineweaver-Burke plot is given as follows:

$$1/[S] = -\frac{1+\frac{[H]}{K_{h2}}}{K_s \cdot (1+\frac{[H]}{K_{h1}})}$$

As long as K_{h1} value is not much different from K_{h2}, the plot converges on the abscissa, a characteristic feature of noncompetitive inhibition.

pH effect of substrate and halide inhibition

The pH dependence of PPO inhibition by halides has been mentioned in previous studies. In the kinetic study of frog epidermis tyrosinase interaction with chloride, enhanced inhibition was also observed at acidic pH (Penafiel et al., 1984). Valero and Garcia-Carmona also described a positive kinetic cooperativity between sodium chloride and catechol in grape PPO at pH 5.0 from their observation of a lag period in product accumulation curves. In another study, Martinez and colleagues showed that the inhibition of iodide and fluoride of tyrosinases from frog epidermis, mushroom, and mouse melanoma (Martinez et al., 1986) was stronger in acidic conditions. The results of our kinetic analysis also show that mPPO inhibition is sensitive to pH. The following scheme is a general description for halide inhibition in acidic conditions:

$$\text{mPPO} \underset{}{\overset{H^+}{\rightleftharpoons}} \text{mPPO*} \overset{X^-}{\rightleftharpoons} \text{mPPO-X}$$

where mPPO* is the protonated form of the enzyme, able to bind the halide inhibitors.

At low pH, halide and a protonable ligand (L) compete for the copper ion at the PPO active site. During enzyme catalysis, the bond between copper and L is weak, and thus easily displaced by the halide. In mPPO, it is proposed that one of the copper-bound histidine residue becomes the protonable ligand that detaches from the copper ion and is replaced by halide. Figure 2.14 offers a simple diagram to illustrate this phenomenon.

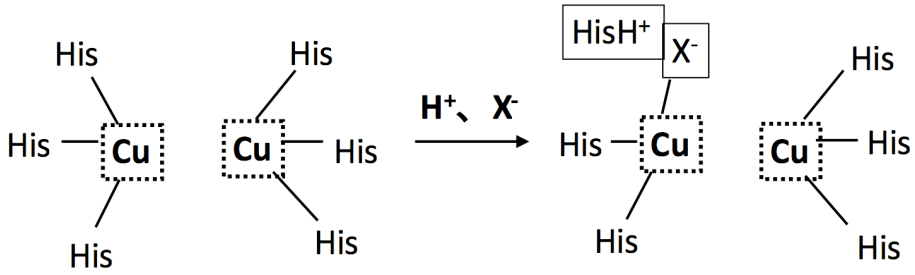

Figure 2.14 Illustration of proposed halide binding to mushroom PPO.
At acidic pH, where inhibition was most evident, a histidine residue is protonated and detaches from the copper ion. The halide inhibitor then binds to PPO at the site vacated by the histidine residue.

The crystal structure of *Agaricus bisporus* tyrosinase reported by Ismaya et al. provides support to the proposed model. It described one histidine residue of the Cu center that can be

the protonable ligand replaced by the inhibitor. From among the six histidine residues bound to the Cu center, only His269 side chain has no direct interactions with other protein ligands, making it more flexible and easier to detach from the active site. Unlike His269, the other copper ligands are tightly bound to other protein residues, either by hydrogen bond or by covalent thioether interactions. This restricts their movement and more so, their replacement by inhibitors (Ismaya et al., 2011).

This model is likewise shared by many authors and thus, can be adapted for further discussions in this paper (Penafiel et al., 1984, Valero and Garcia-Carmona, 1998, Martinez et al., 1986).

Chapter 3 Binding analysis of Halides to mushroom PPO using nuclear magnetic resonance (NMR) and Electrochemical Experiments

As the contents of this chapter are anticipated to be published as a paper in a scholarly journal, it cannot be published online. The paper is scheduled to be published within five years.

Chapter 4 mPPO Inhibition by Disulfide-containing Compounds

As the contents of this chapter are anticipated to be published as a paper in a scholarly journal, it cannot be published online. The paper is scheduled to be published within five years.

Chapter 5 Summary and Conclusion

The reactions of PPO are undesirable from the point of view of agriculture and aesthetics, causing major losses in the nutrition and supply of food. Through this paper, I attempt to contribute to remedy this problem by providing some knowledge on mechanisms governing PPO inhibition.

The kinetic data show that the inorganic halides used in this study are effective in controlling PPO activity. Chloride and bromide decreased PPO activity but did not eliminate it. As much as 20% of activity of the uninhibited enzyme still remained even with a high concentration of chloride and bromide added. Iodide exhibited stronger inhibition power compared to chloride and bromide. Fluoride was the strongest inhibitor among the halides, resulting in an almost total loss of activity even with at a small concentration. The disulfide-containing compounds cystine and HEDS also stopped PPO reaction, but in a time-dependent manner. It was also observed that inhibition of PPO is pH-dependent, where significant loss of activity was observed in pH 5.0.

A Lineweaver-Burke analysis of the kinetic behavior presented that chloride and bromide inhibit mPPO activity via a non-competitive mechanism, able to bind to either the free enzyme or the enzyme-substrate complex. Iodide, on the other hand, prevents enzyme activity uncompetitively. It was also noted that substrate inhibition is experienced by PPO when excess amounts of catechol are present in the solution. Furthermore, substrate inhibition decreases halide inhibition. This suggests that excess substrate and halide compete with each other for binding at the allosteric inhibitory site, Site B. From the derived kinetic constants, it is understood that the binding of bromide and chloride reduces the affinity of substrate to the active site, while the opposite effect happens when iodide was used as inhibitor. The ionic size of the halides may account for the phenomenon since it is believed that the binding of halide to Site B introduces structural changes in the enzyme that affects catechol binding and causes inhibition.

The original contents are anticipated to be published in a scholarly journal and cannot be published online. The paper is scheduled to be published within five years.

The allosteric interaction between the active and inhibitory sites is further supported by the known crystal structure of tyrosinase from *Agaricus bisporus.* The dimers that make up the catalytically significant H-subunit each possess a copper center and in instances that both catechol and halide inhibitor are present in a solution, it can be imagined that catechol binds to the Cu in one subunit and the inhibitor binds to the Cu of the other subunit to cause an inhibition.

In summary, my experiments were conducted following this general model of PPO inhibition:

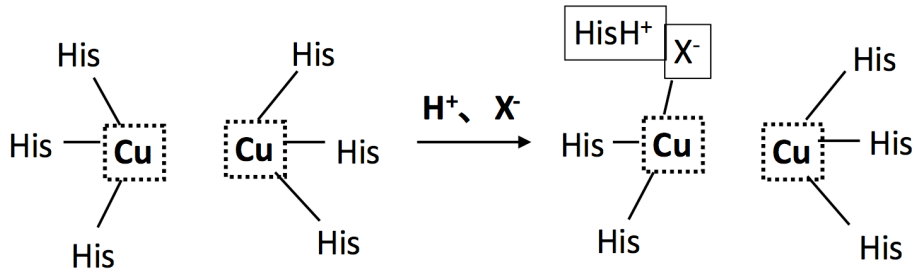

where, at pH 5.0, a histidine residue is protonated and cleaves from the active site Cu. The vacated site now becomes a docking point for inhibitor ligands. With this model in mind, all possible inhibition mechanisms by ligands are dictated by its interaction with Cu. The different properties of Cu enable it to interact with ligands via various mechanisms. For one, it is a redox active species, changing oxidation states in biological systems. The different redox states by Cu makes them amenable to interact with a wide spectrum of ligands. In this case, binding is easily predicted by the HSAB rule where Cu^{+} and Cu^{2+} show distinct binding character individually. It is also a transition metal characterized by available d orbitals. This trait allows Cu to bind covalently with ligands that have valence electrons for sharing. Lastly, it can also act as a charged ion capable of forming ionic interactions. From the combined results of kinetic, electrochemical, and spectroscopic experiments, I conclude that ligand binding to the dinuclear copper may be achieved by any of the following mechanisms:

1. Weak hydrophobic interactions under reducing conditions as exhibited by iodide- Iodide shows uncompetitive inhibition and can bind only when the substrate is bound to PPO. At this stage, Cu is thought to be in the cuprous state. A further evidence is the irreversibility of the reaction in CV. Lastly, the different NMR spectra for the reduced and the oxidized PPO clearly present that iodide has stronger affinity for the reduced enzyme. The preferential affinity of iodide to the reduced Cu is logical, if based on HSAB rules.

2. Weak hydrophobic interactions by chloride and bromide- For ligands that do not have redox character, such as chloride and bromide, ionic size may be the important factor in binding. These halides bound to PPO, indiscriminate of its redox state. Further, the addition of chloride did not affect iodide NMR, which means that it follows a different binding mechanism.

3. Strong ionic interactions that occurs in fluoride binding- Fluoride strongly binds to PPO at pH 5.0 to cause inhibition. The strong binding is further understood from CV data, where the addition of fluoride severely disrupted the electron cloud around Cu, causing the redox peaks to disappear altogether. Since the binding is indiscriminate towards the redox state of the enzyme and exchange with free ions is difficult, it can be concluded that fluoride attachment occurs via a strong ionic interaction with the PPO Cu or with ionizable groups on the protein surface. The pH dependence of the CV results also proves this since ionic groups that are thought to be involved in binding are not as many under neutral conditions.

4. The original contents are anticipated to be published in a scholarly journal and cannot be published online. The paper is scheduled to be published within five years.

The gathered information proves the versatility of PPO in terms of accessibility and reactivity with various inhibitor ligands. It is hopeful for a food scientist as it opens many ways of controlling the activity of this enzyme. On the other end, it can also be taxing as a clear-cut mechanism that applies to all PPOs and all inhibitor ligands is yet to be provided. Although this paper touched only but a surface of the understanding of PPO inhibition, the knowledge gained can be used in the development of potential enzyme inhibitors, both synthetic and from natural sources. I have laid down the optimum conditions that affect inhibition and provided insight that the redox state of PPO can dictate ligand affinity to the enzyme. For my personal research, I intend to expand on this topic by screening natural products from marine and microorganisms and assess its potential use as a PPO inhibitor. As a further application, the new inhibitors gathered may be developed for use in the food industry.

Acknowledgements

I would like to express my sincerest gratitude to the following people who have helped me in my journey through graduate school.

First and foremost, I am deeply indebted to Professor Etsuro Yoshimura, who conceptualized and supervised a major part of this study. I am forever thankful for his willingness to take me under his supervision despite my lack of a solid research foundation when I started. His trust in my capabilities and potentials has given me the courage to continue my research despite major setbacks. By his careful guidance and good example, I received training on how to become a more knowledgeable scientist and a better person. He also instilled in me the value of love for work. I deeply appreciate all his imparted wisdom and concern for the welfare of his students. I will never forget his mentorship and it will serve as my example as I pursue an academic career. If not for his supervision, my research achievements would not have been possible.

My sincerest thanks goes to Dr. Michio Suzuki, whose encouraging words helped regain my confidence to do experiments. He is selfless in sharing his knowledge and expertise with his students. He is also my role model for patience and hardwork. I thank him for taking time out of his busy schedule to closely monitor my experiments and for our discussions. I remember the wise advices he gave when I consulted him about my research career as I start my path in the academe. I deeply appreciate his support and help in the processing of my documents for my dissertation.

Next, with immense gratitude, I acknowledge the help of Dr. Yuki Imura. I thank him for seeing my experiments and for giving insights regarding my study. Although beyond the scope of his work, he assisted me in the numerous reports and essays I had to write in Nihongo. He was also very helpful in the review and improvement of this manuscript. He truly deserves credit for the enormous progress I have achieved in my research.

I consider it an honor to have Professor Haruhiko Masaki, Project Professor Tomiko Asakura, and Associate Professor Koji Nagata as the members of the committee. I am grateful for their willingness to review and assess my manuscript. Their inputs and advice are highly appreciated and is sure to greatly improve my study.

My NMR experiments and study would not have been successful if not for the kind assistance of Associate Professor Kazuo Furihata. He was willing to extend help especially with the principles and operation of the NMR. Although we worked together for only a short time, he trained me well on interpreting the results, and gave me the confidence to conduct my experiments. His patience during my consultations on NMR principles and techniques is most highly appreciated.

I owe a big thanks to my fellow students in the Laboratory of Analytical Chemistry. I thank my seniors who taught me the ropes in the lab and for their kindness in translating many Japanese terms. I am also very grateful for my *kouhais,* for their random acts of kindness and for our small talks that brought joy when I was having difficulties. They will always be a good memory of Japan which I will treasure.

My graduate school dream would definitely be impossible if not for the financial support I received from Ajinomoto Scholarship Foundation, Tsuji Kokusai Scholarship Foundation, and Iwatani Naoji Memorial Foundation. Their support assured me of a comfortable life which allowed me to focus on my study. The numerous activities I enjoyed with them were also my lessons on Japanese culture and cross-cultural relations.

Special thanks also go to The Association of Filipino Students in Japan (AFSJ) and Science and Technology Advisory Council- Japan (STAC-J). My memberships in these organizations not only gave me a chance to get together with my fellow Filipinos in Japan, it also gave me the inspiration to excel and serve the country through Science.

I would like to share all my successes with my family. They stayed with me through all my victories and failures, and made sure I kept a happy disposition in all circumstances. Their constant communication helped me when I was having difficulties living alone.

Lastly, I would like to give the greatest glory to my Almighty God. He is my source of all wisdom and inspiration, and provided strength when I felt that everything was impossible. This dissertation is dedicated to Him.

REFERENCES

Aguey-Zinsou, K.-F., Bernhardt, P. V., De Voss, J. J., & Stessor, K. E. (2003). Electrochemistry of P450 cin: new insights into P450 electron transfer. *Chem. Commun.*, 418-419.

Andersen, S. O., Peter, M. G., & Roepstorff, P. (1996). Cuticular Sclerotization in Insects. *Comp. Biochem. Physiol, 113B*(4), 689-705.

Andersson, T., Thulin, E., & Forsen, S. (1979). Ion Binding to Cytochrome c Studied by Nuclear Magnetic Quadrupole Relaxation. *Biochemistry, 18*(12), 2487-2493.

Arecchi, A., Scampicchio, M., Drusch, S., & Mannino, S. (2010). Nanofibrous membrane based tyrosinase-biosensor for the detection of phenolic compounds. *Analytica Chimica Acta, 659*, 133-136.

Ashraf, Z., Rafiq, M., Seo, S.-Y., Kwon, K. S., Babar, M. M., & Sadaf Zaidi, N.-u.-S. (2015). Kinetic and in silico studies of novel hydroxy-based thymol analogues as inhibitors of mushroom tyrosinase. *European Journal of Medicinal Chemistry, 98*, 203-211.

Banci, L., Bertini, I., Luchinat, C., Scozzafava, A., & Turano, P. (1989). Binding of Fluoride to Copper Zinc Superoxide Dismutase. *Inorganic Chemistry, 28*(12), 2377-2381.

Battaini, G., Monzani, E., Casella, L., Lonardi, E., Tepper, A. W. J. W., Canters, G. W., & Bubacco, L. (2002). Tyrosinase-catalyzed Oxidation of Fluorophenols. *The Journal of Biological Chemistry, 277*, 44606-44612.

Bubacco, L., Salgado, J., Tepper, A. W. J. W., Vijenboom, E., & Canters, G. W. (1999). ^{1}H NMR spectroscopy of the binuclear Cu(II) active site of *Streptomyces antibioticus* tyrosinase. *FEBS Letters, 442*, 215-220.

Bubacco, L., Vijenboom, E., Gobin, C., Tepper, A. W. J. W., Salgado, J., & Canters, G. (2000). Kinetic and paramagnetic NMR investigations of the inhibition of *Streptomyces antibioticus* tyrosinase. *Journal of Molecular Catalysis B, Enzymatic 8*, 27-35.

Chakraborty, P., Majumder, I., Kara, H., Chattopadhyay, S. K., Zangrando, E., & Das, D. (2015). Azido bridged mediated catecholase actiivty, electrochemistry and magnetic behavior of a dinuclear copper (II) complex of a phenol based "end-off" compartment ligand. *Inorganica Chimica Acta, 436*, 139-145.

Chen, J. S., Wei, C.-i., & Marshall, M. R. (1991). Inhibition Mechanism of Kojic Acid on Polyphenol Oxidase. *Journal of Agricultural and Food Chemistry, 39*(11), 1897-1901.

Chen, J. S., Wei, C.-i., Rolle, R. S., Otwell, W. S., Balaban, M. O., & Marshall, M. R. (1991). Inhibitory Effect of Kojic Acid on Some Plant and Crustacean Polyphenol Oxidases. *J. Agric. Food Chem., 39*, 1396-1401.

Chen, Q.-X., & Kubo, I. (2002). Kinetics of Mushroom Tyrosinase Inhibition by Quercetin. *J. Agric. Food Chem., 50*, 4108-4112.

Chiancone, E., Norne, J.-E., & Forsen, S. (1981). The Use of NMR Spectroscopy in Studies of Ion Binding to Hemoglobin. *Methods in Enzymology, 76*, 552-559.

Decker, H., Ryan, M., Jaenicke, E., & Terwilliger, N. (2001). SDS-Induced Phenolxidase Activity of Hemocyanins from *Limulus polyphemus*, *Eurypelma californicum*, and Cancer magister *The Journal of Biological Chemistry, 276*(21), 17796-17799.

Decker, H., Schweikardt, T., Nillius, D., Salzbrunn, U., Jaenicke, E., & Tuczek, F. (2007). Similar enzyme activation and catalysis in hemocyanins and tyrosinases. *Gene, 398*, 183-191.

Decker, H., Schweikardt, T., & Tuczek, F. (2006). The First Crystal Structure of Tyrosinase: All Questions Answered? *Angew. Chem. Int. Ed., 45*, 4546-4550.

Diwakar, S. K., & Mishra, S. K. (2011). Purification and Biochemical Characterization of Ionically Unbound Polyphenol Oxidase from *Musa paradisiaca* Leaf. *Preparative Biochemistry and Biotechnology, 41*, 187-200.

Eicken, C., Zippel, F., Buldt-Karentzopoulos, K., & Krebs, B. (1998). Biochemical and spectroscopic characterization of catechol oxidase from sweet potatoes (*Ipomoea batatas*) containing a type-3 dicopper center. *FEBS Letters, 436*, 293-299.

Fleming, B. D., Tian, Y., Bell, S. G., Wong, L.-L., Urlacher, V., & Hill, H. A. O. (2003). Redox properties of cytochrome P450 BM3 measured by direct methods. *Eur. J. Biochem, 270*, 4082-4088.

Gan, C., Cui, J., Su, S., Lin, Q., Jia, L., Fan, L., & Huang, Y. (2014). Synthesis and antiproliferative activity of some steroidal thiosemicarbazones, semicarbazones and hydrazones. *Steroids, 87*, 99-107.

Gawande, S. S., Warangkar, S. C., Bandgar, B. P., & Khobragade, C. N. (2013). Synthesis of new heterocyclic hybrids based on pyrazole and thiazolidinon scaffolds as potent inhibitors of tyrosinase. *Bioorganic and Medicinal Chemistry, 21*, 2772-2777.

Halaouli, S., Asther, M., Kruus, K., Guo, L., Hamdi, M., Sigoillot, J. C., . . . Lomascolo, A. (2005). Characterization of a new tyrosinase from *Pycnoporus* species with high potential for food technological applications. *Journal of Applied Microbiology, 98*, 323-343.

Halle, B., & Lindman, B. (1978). Chloride Ion Binding to Human Plasma Albumin from Chlorine-35 Quadrupole Relaxaion. *Biochemistry, 17*(18), 3774-3780.

Hiestand, P. C., & Strasser, M. (1985). Immunodilating Activities of Ethylene-2,2'-Bis(Dithio)Bis(Ethanol) and Related Compounds: Effects in Murine Lymphocyte Proliferation and Functions in vitro. *Int. J. Immunopharmac., 7*(1), 129-140.

Himmelwright, R. S., Eickman, N. C., LuBien, C. D., Lerch, K., & Solomon, E. I. (1980). Chemical and Spectroscopic Studies of the Binuclear Copper Active Site of *Neurospora* Tyrosinase: Comparison to Hemocyanins. *Journal of American Chemical Society, 102*, 7339-7344.

Honeychurch, M. (2006). The direct electrochemistry of cytochrome P450. What are we actually measuring?1-15.

Hoogvliet, J. C., Lievense, L. C., van Dijk, C., & Veeger, C. (1988). Electron transfer between the hydrogenase from *Desulfovibrio vulgaris* (Hildenborough) and violegens. *Eur. J. Biochem, 174*, 273-280.

Hosseini-Yazdi, S. A., Hosseinpour, S., & Khandar, A. A. (2015). Copper (II) and nickel (II) complexes with two new bis(thiosemicarbazone) ligands: Synthesis, characterization, X-ray crystal structures and their electrochemistry behavior. *Inorganica Chimica Acta, 427*, 124-130.

Inamdar, S., Joshi, S., Bapat, V., & Jadhav, J. (2014). Purification and Characterization of RNA Allied Extracellular Tyrosinas from *Aspergillus* Species. *Applied Biochemistry and Biotechnology, 172*(3), 1183-1193.

Ionita, E., Aprodu, J., Stanciuc, N., Rapeanu, G., & Bahrim, G. (2014). Advances in structure-function relationships of tyrosinase from *Agaricus bisporus*- Investigation on heat-induced conformational changes. *Food Chemistry, 156*, 129-136.

Ismaya, W. T., Rozeboom, H. J., Wejin, A., Mes, J. J., Fusetti, F., Wichers, H. J., & Dijkstra, B. W. (2011). Crystal Structure of *Agaricus bisporus* Mushroom Tyrosinase: Identity of the Tetramer Subunits and Interaction with Tropolone. *Biochemistry, 50*, 5477-5486.

Jackman, M.P., Hajnal, A. & Lerch, K. (1991). Albino mutants of *Streptomyces glaucescens* tyrosinase. *Biochem.*, *274*, 707-713.

Jaenicke, E., & Decker, H. (2004). Functional Changes in the Family of Type 3 Copper Proteins During Evolution. *ChemBioChem, 5*, 163-169.

Janovitz-Klapp, A. H., Richard, F. C., Goupy, P. M., & Nicolas, J. J. (1990). Inhibition Studies on Apple Polyphenol Oxidase. *J. Agric. Food Chem., 38*(4), 926-931.

Kahn, V. (1985). Effects of Proteins, Protein Hydrozylates and Amino acids on o-Dihydroxyphenolase Activity of Polyphenol Oxidase of Mushroom, Avocado, and Banana. *Journal of Food Science, 50*, 111-115.

Kaintz, C., Mauracher, S. G., & Rompel, A. (2014). Type-3 Copper Proteins: Recent Advances on Polyphenol Oxidases. *Advances in Protein Chemistry and Structural Biology, 97*, 1-35.

Karlin, K. D., Zhang, C. X., Rheingold, A. L., Galliker, B., Kaderli, S., & Zuberbuhler, A. D. (2012). Reversible dioxygen binding and arene hydroxylation reactions: Kinetic and Thermodynamic studies involving ligand electronic and structural variations. *Inorganica Chimica Acta, 389*, 138-150.

Kermasha, S., Goetghebeur, M., & Monfette, A. (1993). Studies on Inhibition of Mushroom Polyphenol Oxidase Using Chlorogenic Acid as Substrate. *J. Agric. Food Chem., 41*, 526-531.

Kermasha, S., Goetghebeur, M., Monfette, A., Metche, M., & Rovel, B. (1993). Inhibitory Efects of Cysteine and Aromatic Acids on Tyrosinase Activity. *Phytochemistry, 34*(2), 349-353.

Klabunde, T., Eicken, C., Sacchettini, J. C., & Krebs, B. (1998). Crystal structure of a plant catechol oxidase containing a dicopper center. *Nature Structural Biology, 5*(12), 1084-1090.

Kubo, I., Kinst-Hori, I., Chaudhuri, S. K., Kubo, Y., Sanchez, Y., & Ogura, T. (2000). Flavonols from *Heterotheca inuloides*: Tyrosinase Inhibitory Activity and Structural Criteria. *Bioorganic & Medicinal Chemistry, 8*, 1749-1755.

Kujipers, T. F. M., Gruppen, H., Sforza, S., van Berkel, W. J. H., & Vincken, J.-P. (2013). The antibrowning agent sulfite inactivates *Agaricus bisporus* tyrosinase through covalent modification of the copper- B site. *FEBS Journal, 280*, 6184-6195.

Lachowicz, J. I., Nurchi, V. M., Crisponi, G., Jaraquemada Pelaez, M. d. G., Rescigno, A., Stefanowicz, P.,Szewczuk, Z. (2015). Metal coordination and tyrosinase inhibition studies with Kojic-B-Ala-Kojic. *Journal of Inorganic Biochemistry, 151*, 36-43.

Laino, A., Lavarias, S., Suarez, G., Lino, A., & Cunningham, M. (2015a). Characterization of Phenoloxidase Activity from Spider *Polybetes pythagoricus* Hemocyanin. *J. Exp. Zool., 323A*, 547-555.

Lewis, D. E. V., & Hlavica, P. (2000). Interactions between redox partners in various cytochrome P450 systems: Fundamental and structural aspects. *Biochimica et Biophysica Acta, 1460*, 353-374.

Li, J., Zhang, D., Ward, K. M., Prendergast, G. C., & Ayene, I. S. (2012). Hydroxyethyl disulfide as an efficient metabolic assay for cell viability in vitro. *Toxicology in Vitro, 26*(26), 603-612.

Lim, G. G. F., Imura, Y., & Yoshimura, E. (2012). Substrate Inhibition Competes with Halide Inhibition in Polyphenol Oxidase.*Protein Journal, 31*, 609-614.

Lindman, B. (1978). Applications of Quadrupolar Effects in NMR for Studies of Ion Binding in Biological and Model Systems. *Journal of Magnetic Resonance, 32*, 39-47.

Loncar, N., & Vujcic, Z. (2011). Tentacle carrier for immobilization of potato phenoloxidase and its application for halogenophenols removal from aqueous solutions. *Journal of Hazardous Materials, 196*, 73-78.

Lund, M., Vacha, R., & Jungwirth, P. (2008). Specific Ion-Binding to Macromolecules: Effects of Hydrophobicity and Ion Pairing. *Langmuir, 24*(7), 3387-3391.

Martinez, J. H., Solano, F., Penafiel, R., Galindo, J. D., Iborra, J. L., & Lozano, J. A. (1986). Comparative Study of Tyrosinases from Different Sources: Relationship between Halide Inhibition and the Enzyme Active Site. *Comp. Biochem. Physiol., 83B*(3), 633-636.

Martinez, M. V., & Whitaker, J. R. (1995). The biochemistry and control of enzymatic browning. *Trends in Food Science & Technology, 6*, 195-200.

Marusek, C. M., Trobaugh, N. M., Flurkey, W. H., & Inlow, J. K. (2006). Comparative analysis of polyphenol oxidase from plant and fungal species. *Journal of Inorganic Biochemistry, 100*, 108-123.

Marwedel, B. J., & Kurland, R. J. (1975). Fluoride Ion as a NMR Relaxation Probe of Paramagnetic Metalloenzymes: The Binding of Fluoride to Galactose Oxidase. *Biochemical and Biophysical Research Communications, 63*(3), 773-779.

Mendes, E., Perry, M. d. J., & Francisco, A. P. (2014). Design and Discovery of mushroom tyrosinase inhibitors and their therapeutic applications. *Expert Opin. Drug Discov., 9*(5), 533-554.

Mizukoshi, Y., Abe, A., Takizawa, T., Hanzawa, H., Fukunishi, Y., Shimada, I., & Takahashi, H. (2012). An Accurate Pharmacophore Mapping Method by NMT Spectroscopy. *Angew. Chem. Int. Ed., 51*, 1362-1365.

Munoz, J. L., Garcia-Molina, F., Varon, R., Rodriguez-Lopez, J. N., Garcia-Canovas, F., & Tudela, J. (2006). Calculating molar absoptivities for quinones: Application to the measurement of tyrosinase activity. *Analytical Biochemistry, 351*, 128-138.

Nagai, T., Osaki, T., & Kawabata, S.-i. (2001). Functional Conversion of Hemocyanin to Phenoloxidase by Horseshoe Crab Antimicrobial Peptides. *The Journal of Biological Chemistry, 276*(29), 27166-27170.

Norne, J.-E., Hjalmarsson, S.-G., Lindman, B., & Zeppezauer, M. (1975). Anion Binding Properties of human Serum Albumin from Halide Ion Quadrupole Relaxation. *Biochemistry, 14*(15), 3401-3407.

Nozue, M., Arakawa, D., Iwata, Y., Shioiri, H., & Kojima, M. (1999). Activation by Proteolysis *in vivo* of 60-ku Latent Polyphenol Oxidases in Sweet Potato Cells in Suspension Culture. *J. Plant Physiol., 155*, 297-301.

Oz, F., Colak, A., Ozel, A., Sag, N., Ertunga, L., & Sesli, E. (2013). Purification and Characterization of a Mushroom Polyphenol Oxidase and Its Activity in Organic Solvents. *Journal of Food Biochemistry, 37*, 36-44.

Park, J. W., Dec, J., Kim, J. E., & Bollag, J.-M. (1999). Effect of Humic Constituents on the Transformation of Chlorinated Phenols and Anilines in the Presence of Oxidoreductive Enzymes or Birnessite. *Environ. Sci. Technol., 33*, 2028-2034.

Park, J. W., Dec, J., Kim, J. E., & Bollag, J. M. (2000). Dehalogenation of Xenobiotics as a Consequence of Binding to Humic Materials. *Arch. Environ. Contam. Toxicol., 38*, 405-410.

Park, Y.-D., Kim, S.-Y., Lyou, Y.-J., Lee, J.-Y., & Yang, J.-M. (2005). A new type of uncompetitive inhibition of tyrosinase induced by Cl-binding. *Biochimie, 87*, 931-937.

Parvez, S., Kang, M., Chung, H.-S., & Bae, H. (2007). Naturally Occurring Tyrosinase Inhibitors: Mechanism and Applications in Skin Health, Cosmetics, and Agriculture Industries. *Phytotherapy Research, 21*, 805-816.

Pate, J. E., Ross, P. K., Thamann, T. J., Reed, C. A., Karlin, K. D., Sorell, T. N., & Solomon, E. I. (1989). Spectroscopic Studies of the Charge Transfer and Vibrational Features of Binuclear Copper (II) Azide Complexes: Comparison to the Coupled Binuclear Copper Active Site in Met Azide Hemocyanin and Tyrosinase *Journal of American Chemical Society, 111*(14), 5198-5209.

Paul, B., & Gowda, L. R. (2000). Purification and Characterization of a Polyphenol Oxidase from the Seeds of Field Bean (*Dolichos lablab*). *J. Agric. Food Chem, 48*, 3839-3846.

Pearson, R. G. (1968). Hard and Soft Acids and Bases, HSAB, Part 1. *Journal of Chemical Education, 45*(9), 581-587.

Pearson, R. G. (1968). Hard and Soft Acids and Bases, HSAB, Part II. *Journal of Chemical Education, 45*(10), 643-648.

Penafiel, R., Galindo, J. D., Solano, F., Pedreno, E., Iborra, J. L., & Lozano, J. A. (1984). Kinetic Study of the Interaction Between Frog Epidermis Tyrosinase and Chloride. *Biochimica et Biophysica Acta, 788*, 327-332.

Pizzocaro, F., Torreggiani, D., & Gilardi, G. (1993). Inhibition of Apple Polyphenoloxidase (PPO) by Ascorbic Acid, Citric Acid, and Sodium Chloride *Journal of Food Processing and Preservation, 17*, 21-30.

Pless, D. D., Aguilar, M. B., Falcon, A., Lozano-Alvarez, E., & Heimer de la Cotera, H. (2003). Latent phenoloxidase activity and N-terminal amino acid sequence of hemocyanin from *Bathynomus giganteus*, a primitve crustacean. *Archives of Biochemistry and Biophysics, 409*, 402-410.

Queiroz, C., Mendes Lopes, M. L., Fialho, E., & Valente-Mesquita, V. L. (2008). Polyphenol Oxidase: Characteristics and Mechanisms of Browning Control. *Food Reviews International, 24*, 361-375.

Ramsden, C. A., & Riley, P. A. (2014). Tyrosinase: The four oxidation states of the active site and their relevance to enzymatic activation, oxidation and inactivation. *Bioorganic and Medicinal Chemistry, 22*(2388-2395).

Raynova, Y., Todinova, S., Yordanov, D., & Idakieva, K. (2014). SDS-induced phenoloxidase activity of *Helix aspersa* maxima hemocyanin. *Bulgarian Chemical Communications, 46*(Special Issue A), 111-116.

Rescigno, A., Sollai, F., Pisu, B., Rinaldi, A., & Sanjust, E. (2002). Tyrosinase Inhibition; General and Applied Aspects. *Journal of Enzyme Inhibition and Medicinal Chemistry, 17*, 207-218.

Reyes-Caballero, H., Campanello, G. C., & Giedroc, D. P. (2011). Metalloregulatory proteins: Metal selectivity and allosteric switching. *Biophysical Chemistry, 156*, 103-114.

Richard-Forget, F. C., Goupy, P. M., & Nicolas, J. J. (1992). Cysteine as an Inhibitor of Enzymatic Browning. 2. Kinetic Studies. *J. Agric. Food Chem, 40*, 2108-2113.

Richard-Forget, F. C., Rouet-Mayer, M.-A., Goupy, P. M., Philippon, J., & Nicolas, J. J. (1992). Oxidation of Chlorogenic Acid, Catechins, and 4-Methylcatechol in Model Solutions by Apple Polyphenol Oxidase. *J. Agric. Food Chem, 40*, 2114-2122.

Robinson, S. P., & Dry, I. B. (1992). Broad Bean Leaf Polyphenol Oxidase is a 60-Kilodalton Protein Susceptible to Proteolytic Cleavage. *Plant Physiol., 99*, 317-323.

Rompel, A., Buldt-Karentzopoulos, K., Molitor, C., & Krebs, B. (2012). Purification and spectroscopic studies on catechol oxidase from lemon balm (*Melissa officinalis*). *Phytochemistry, 81*, 19-23.

Rompel, A., Fischer, H., Meiwes, D., Buldt-Karentzopoulos, K., Dillinger, R., Tuczek, F., Krebs, B. (1999). Purification and spectroscopic studies on catechol oxidase from *Lycopus europaeus* and *populus nigra*: Evidence for a dinuclear copper center of type-3 and spectroscopic similarities to tyrosinase and hemocyanin. *JBIC, 4*, 56-63.

Sakurada, J., Takahashi, S., Shimizu, T., Hatano, M., Nakamura, S., & Hosoya, T. (1987). Proton and iodine-127 Nuclear Magnetic Resonance Studies on the Binding of Iodide by Lactoperoxidase. *Biochemistry, 26*, 6478-6483.

Salvato, B., Santamaria, M., Beltramini, M., Alzuet, G., & Casella, L. (1998). The Enzymatic Properties of *Octopus vulgaris* Hemocyanin: o-diphenol Oxidase Activity. *Biochemistry, 37*, 14065-14077.

Sanchez-Ferrer, A., Rodriguez-Lopez, J. N., Garcia-Canovas, F., & Garcia-Carmona, F. (1995). Tyrosinase: a comprehensive review of its mechanism. *Biochimica et Biophysica Acta, 1247*, 1-11.

Sanders II, C., & Tsai, M.-D. (1989). Ligand-Protein Interactions via Nuclear Magnetic Resonance of Quadrupolar Nuclei. *Methods in Enzymology, 177*, 317-333.

Seo, S.-Y., Sharma, V. K., & Sharma, N. (2003). Mushroom Tyrosinase: Recent Prospects. *Journal of Agricultural and Food Chemistry, 51*, 2837-2853.

Severini, C., Baiano, A., De Pilli, T., Romaniello, R., & Derossi, A. (2003). Prevention of enzymatic browning in sliced potatoes by blanching in boiling saline solutions. *Lebensm.-Wis.u.-Technol., 36*, 657-665.

Shleev, S., Tkac, J., Christenson, A., Ruzgas, T., Yaropolov, A. I., Whittaker, J. W., & Gorton, L. (2005). Direct electron transfer between copper-containing proteins and electrodes. *Biosensors ans Bioelectronics, 20*, 2517-2554.

Suefuji, K., Lin, S.-J., Wakagi, T., Matsuzawa, H., & Yoshimura, E. (2002). Sodium-23 and Lanthanum-139 Nuclear Magnetic Resonance Studies of Cation Binding to Aqualysin I, a Thermostable Serine Protease. *Biosci. Biotechnol. Biochem., 66*(6), 1281-1286.

Tepper, A. W. J. W., Bubacco, L., & Canters, G. W. (2002). Structural Basis and Mechanism of the Inhibition of the Type-3 Copper Protein Tyrosinase from *Streptomyces antibioticus* by Halide Ions. *The Journal of Biological Chemistry, 277*(34), 30436-30444.

Unal, M. U. (2007). Properties of polyphenol oxidase from Anamur banana (*Musa cavendishii*). *Food Chemistry, 100*, 909-913.

Valdez, C. E., smith, Q. A., Nechay, M. R., & Alexandrova, A. N. (2014). Mysteries of Metals in Metalloenzymes. *Accounts of Chemical Research, 47*, 3110-3117.

Valero, E., & Garcia-Carmona, F. (1998). pH-dependent Effect of Sodium Chloride on Latent Grape Polyphenol Oxidase. *J. Agric. Food Chem, 46*, 2447-2451.

Vamos-Vigyazo. Prevention of Enzymatic Browning in Fruits and Vegetables. In *Enzymatic Browning and Its Prevention*.

van Gastel, M., Bubacco, L., Groenen, E. J. J., Vijenboom, E., & Canters, G. W. (2000). EPR study of the dinuclear active copper site of tyrosinase from *Streptomyces antibioticus FEBS Letters, 474*, 228-232.

Viglino, P., Rigo, A., Stevanato, R., & Ranieri, G. A. (1979). The Binding of Fluoride Ion to Bovine Cuprozinc Superoxide Dismutase as Studied by ^{19}F Magnetic Relaxation. *Journal of Magnetic Resonance, 34*, 265-274.

Waite, J. H. (1976). Calculating Extinction Coefficients for Enzymatically Produced o-Quinones. *Analytical Biochemistry, 75*, 211-218.

Wen, Z., Ye, B., & Zhou, X. (1997). Direct Electron Transfer Reaction of Glucose Oxidase at Bare Silver Electrodes and Its Application in Analysis. *Electroanalysis, 9*(8), 641-644.

Whitaker, J. R., & Lee, C. Y. (1995). Recent Advances in Chemistry of Enzymatic Browning. In A. C. Society (Ed.).

Wilcox, D. E., Porras, A. G., Hwang, Y. T., Lerch, K., Winkler, M. E., & Solomon, E. I. (1985). Substrate Analogue Binding to the Coupled Binuclear Copper Active Site in Tyrosinase. *J. Am. Chem. Soc., 107*, 4015-4027.

Xie, J., Dong, H., Yu, Y., & Cao, S. (2016). Inhibitory Effect of Synthetic aromatic heterocycle thiosemicarbazone derivatives on mushroom tyrosinase: Insights from fluorecence, ^{1}H NMR titration and molecular docking studies. *Food Chemistry, 190*, 709-716.

Xu, F. (1996). Oxidation of Phenols, Anilines, and Benzenethiols by Fungal Laccases: Correlation between Activity and Redox Potentials as well as Halide Inhibition. *Biochemistry, 35*, 7608-7614.

Xu, F., Shin, W., Brown, S. H., Wahleithner, J. A., Sundaram, U. M., & Solomon, E. I. (1996). A study of a series of recombinant fungal laccases and biliburin oxidase that exhibit significant differences in redox potential, substrate specificity, and stability. *Biochimica et Biphysica Acta, 1292*, 303-311.

Yaropolov, A. I., Kharybin, A. N., Emneus, J., Marko-Varga, G., & Gorton, L. (1996). Electrochemical properties of some copper-containing oxidases. *Bioelectrochemistry and Bioenergetics, 40*, 49-57.

Ye, B., & Zhou, X. (1997). Direct electrochemical redox of tyrosinase at silver electrodes. *Talanta, 44*, 831-836.

Yoshimura, E., Tachibe, M., Mori, S., & Yamazaki, S. (2000a). Anion Binding to Porcine Pancreatic alpha-amylase as Probed by Bromine-81 Nuclear Magnetic Resonance Spectrometry. *Spectroscopy Letters, 33*(6), 893-899.

Zocca, F., Lomolino, G., & Lante, A. (2010). Antibrowning potential of *Brassicacaea* processing water. *Bioresource Technology, 101*(10), 3791-3795.